

C.P. No. 189

(16,902)

A R C Technical Report



MINISTRY OF SUPPLY

AERONAUTICAL RESEARCH COUNCIL

CURRENT PAPERS

Shadowgraphs of Model Projectiles Fired at High Mach
Numbers and near $M=1$ in the N.P.L. Ballistic Range

By

W F. Cope, M.A., A.F.R.Ae.S.

of the Aerodynamics Division, N.P.L.

LONDON HER MAJESTY'S STATIONERY OFFICE

1955

FIVE SHILLINGS NET

Shadowgraphs of Model Projectiles Fired at High Mach Numbers
and near $M = 1$ in the N.P.L. Ballistic Range

- By -

W. F. Cope, M.A., A.F.R.Ae.S.
of the Aerodynamics Division, N.P.L.

2nd July, 1954.

SUMMARY

Shadowgraphs of 20 mm projectiles fired in the N.P.L. Ballistic Range at Mach numbers (mainly) above 3 are shown, and the important features discussed.

Shadowgraphs of three rounds whose Mach numbers passed through $M = 1$ in their passage down the range are also shown. In all three cases the drag and in one all the Aerodynamic Force Coefficients were determined. The effect of the retardation is discussed and it is concluded that the effect is probably small enough to be negligible except perhaps on the drag.

These rounds were stable, the unstable region for projectile is at a lower Mach number (about $\frac{3}{4}$). To illustrate this, the analysis of some earlier rounds is included.

Introduction

Before the Ballistic Range of the former Engineering Division, N.P.L. was transferred to Aerodynamics Division, N.P.L. and closed down, several spin stabilized projectiles were fired with muzzle velocities such that the projectile dropped through the velocity of sound in its passage down the range. The rounds were fired to obtain information of value to External Ballisticians. But because of the interest in phenomena in the Transonic Region shown by Aerodynamicists this report has been communicated in case it has anything of value to them.

A selection of the prints from shadowgraphs of projectiles at relatively high Mach numbers (about $3\frac{1}{2}$) have been included in this report because relatively few seem to have been published. Prints of the transonic rounds are also included since these have an interest in their own right. But the emphasis in the case of the latter is rather different because the several aerodynamic force coefficients were determined from the ascertained motion. This involves consideration of both the stability of the motion and of the question of the effect of the acceleration terms. Some transonic rounds fired much earlier have also been included in this section.

TABLE

TABLE

Projectile Number	Length of Body Calibres	Length of Head Calibres	Head Shape C.R.H.	Figure Number	U ft/sec	M	R Millions
F.117	2.50	2.69	7.5	1	1,136	1.009	2.3
				2	1,128	1.002	
				3	1,124	0.998	
				4	1,116	0.991	
				5	1,113	0.988	
F.121	2.50	2.69	7.5	6	1,123	1.000	2.3
				7	1,120	0.997	
				8	1,119	0.996	
				9	1,118	0.995	
				10	1,118	0.995	
F.119	2.50	2.69	7.5	11*	1,131	1.005	2.3
				12*	1,114	0.990	
F.102	2.50	2.69	7.5	13*	2,100	1.86	4.3
F.105				14	2,090	1.84	
F.108	2.50	2.69	7.5	15	3,120	2.75	6.3
F.112				16	3,120	2.76	
I.104	3.02	1.66	3.0	17	3,450	3.08	7.0
I.107				18*	3,480	3.09	
E.101	2.50	2.18	5.0	19	3,480	3.10	7.0
E.103				20*	3,510	3.12	
O.100	2.50	2.18	5/10	21	3,500	3.10	7.0
O.103				22	3,510	3.12	
3A	1.99	2.69	7.5	23	3,510	3.11	7.0
6A				24*	3,500	3.10	
F.114	2.50	2.69	7.5	25	3,510	3.11	7.0
F.115				26*	3,510	3.12	
N.101	2.50	2.18	5/∞	27	3,500	3.10	7.0
N.102			Cone 12.92° semi angle	28*	3,580	3.19	

Calibre of Projectiles

20 mm.

Rifling of Gun

1 turn in 513.4 mm (1.685 ft), nominal 1 in 25.

*

Rounds with appreciable yaw. The plane of the yaw is approximately parallel to the plane of the shadowgraph.

X/Y C.R.H.

Calibre Radius Head

Means a head of length appropriate to a tangential (or true) ogive of X calibres, the radius of the ogive being Y calibres. A tangential ogive head X/X C.R.H. is usually written X C.R.H. and a conical head X/∞ C.R.H. is often specified by its angle.

R/

R

Is calculated with the length (l) of the projectile as the representative length.
 $R \approx 400 \times \text{length in calibres} \times U \text{ ft/sec.}$

The velocity for F.117, F.119 and F.121 was measured on a 3 ft base embracing the frame of the shadowgraph. The distance was known to 0.001 ft and the time to $1 \mu\text{s}$, the velocity is therefore accurate to about 1 part in 3,000. For all the other projectiles the velocity given is the mean value between the first and last frames (about 110 ft). The difference between the velocities at these two frames is between 50 ft/sec and 100 ft/sec depending of course on the retardation.

Shadowgraphs

The Table and its accompanying notes gives the essential information about the rounds fired. The comments which follow will be confined to unusual or striking features revealed and for this reason a number of the shadowgraphs are not explicitly mentioned in the text. As a general comment the boundary layer is clearly defined and it is obvious that it is turbulent towards the base, but it is not possible to say precisely where transition occurs.

The thickening of the boundary layer on the leeward side of the projectile when there is appreciable yaw is well shown in Figs. 4, 11, 14, 16 and 28. The peripheral velocity of the projectile is over 400 f.s. at the highest velocities and the polar diagram of boundary layer thickness cannot be determined from two shadowgraphs at right angles. Therefore it is not known for certain whether the planes of maximum yaw and of maximum thickness coincide. The rifling of the gun is right handed so that the circumferential motion at the top is towards the reader when the nose of the projectile is to his right. In Fig. 27 the thickness of the boundary layer near the shoulder differs markedly on the two sides though there is no yaw in the plane of the shadowgraph and only 5° (at most) in the plane at right angles to it. This is the only case of its kind discovered in about 1,000 shadowgraphs and it is just possible that it is evidence of a phase difference between maximum yaw and maximum boundary thickness. But it seems much more likely that the cause is a slightly bent or eccentric point to the cone.

In Fig. 18 wavelets can be seen on the windward side which appear to originate from the surface near the nose and to be reflected from the head shock so that finally they are almost parallel to the body of the projectile.

In several of the shadowgraphs and in particular in Fig. 21, which is the best example, wavelets can be seen in the region between the head and tail shocks. These wavelets are nearly at right angles to the main flow and their origin is unknown.

In Figs. 4 and 5 the nearly straight shocks at the base of the projectile may be due to gun blast.

In Fig. 27 the total angle of the head shock is about 46° and agrees reasonably well with the predictions of the Maccoll-Taylor theory.

The shadowgraphs were taken by spark, its total duration was about $1 \mu\text{s}$ but the intensity-time curve has a very sharp peak and the effective time is about $0.1 \mu\text{s}$. The source is 1 mm dia. about $4.2''$ from the projectile, the angle of divergence of the beam therefore is about 1 : 100 each side the mean.

Transonic/

Transonic Rounds

(a) Stability

Three projectiles were fired; in one case (F.117) shadowgraphs of the projectile were taken and the drag only determined, in the second (F.121) the course of the head shock at speeds below that of sound was studied as well, and in the third the motion was fully analyzed and all the aerodynamic force coefficients determined. The definitions and the method of analysis will be found in Chapter XIII of Modern Developments, High Speed Flow (1953). The results obtained are as follows:-

Aerodynamic Force Coefficients

Round Number	Average Mach No. \bar{M}	Average Yaw $\bar{\delta}$	Drag, f_D $R/\rho U^2 r^2$	Lift, f_L $L/\rho U^2 r^2 \sin \delta$	Moment, f_M $M/\rho U^2 r^3 \sin \delta$	Yawing Moment f_H $H/\rho U r^4$	Magnus Couple f_J $J/\rho U N r^4 \sin \delta$
F.117	0.998	-	0.746				
F.119	0.996	12.4	0.986	3.67	11.26	82.6	-1.33
F.121	0.995	-	0.681				

wherein, in addition to the symbols already defined:-

$\rho \equiv$ density, $r \equiv$ radius of projectile, $\delta \equiv$ yaw, ω resultant transverse angular velocity of body, $N \equiv$ spin and R, L, M, H and J are respectively the forces or moments (about the C.G. of the projectile) involved in the several definitions.

In all cases the velocity of the projectile drops through that of sound in its passage down the range but, as Figs. 29, 30 and 32 show, there is no discontinuity in the slope of the velocity time curve. The mean yaw of round F.117 may be greater than that of F.121 but there is no way of knowing. The largest yaw visible (in Fig.5 F.117) is about 8° in the plane of the shadowgraph, in Figs. 3 and 4 (F.117) the yaw is about 5° and in Figs. 1 and 2 (F.117) quite small. The yaw in Fig. 6 (F.121) is not more than 3° . The standard ballistic formula $f_R \delta = f_{R0} \left(1 + \frac{\delta^2}{200} \right)$ gives 7.9° and 6.5° for the mean yaws of projectiles F.117 and F.121 respectively and a value of 0.57 for f_{R0} . But the accuracy of this formula in this region is quite unknown and this result only indicates reliably that f_{R0} is in the region of 0.6.

It should be noted that in Figs. 29, 30 and 32 the plotted points are not velocities at a measuring frame but at points approximately midway between. The accuracy (as given in the notes to the Table) is such that the velocity is known to better than 1 f.s.

The distance of the head shock from the nose up to the point where it passes off the plate is plotted as Fig. 31. The distance is calculated on the assumption that the shock is axisymmetrical and that the tangent lines to it, from the spark source, are tangential at points not far from the trajectory. The discrepancy between the Horizontal and Vertical plates in frames 8, 9, 10 and 11 may be due to a breakdown of these assumptions. Two and sometimes more head shocks appear in Figs. 7-10, presumably those nearer to the nose and weaker are reflected shocks from the walls of the range or from tables, cupboards in it. Fig. 31 shews that these shocks do not unite until the projectile is travelling at a speed considerably below that of sound.

The chain dashed line in Fig. 31 indicates the distance separating the projectile and a point moving with constant velocity equal to that of the projectile at time 0. ($M \approx 1.007$, $U \approx 1,128$ ft/sec). It suggests that the observed head shock distances are dependent upon the retardation of the projectile even before $M = 1$. It is of course obvious that the ballistic range and the wind tunnel techniques are not measuring the same quantities because in the former case the body under observation is being retarded. There is a mass of evidence that at Mach numbers far from unity the difference is of no practical importance. The point of Fig. 31 is that it shows that the difference may be appreciable at Mach numbers very near to unity.

The value of f_R may be affected both by the finite size of the range and because the measurements were made with accelerations present. It seems very unlikely that the former is important except almost literally at $M = 1$ because the area ratio range/projectile exceeds 10^4 .

The yawing and C.G. motion of round F.119 are plotted as Figs. 34 and 35 respectively and it can be seen that the round is stable though the damping is not large. The process of analysis revealed that there was no perceptible change in the damping factors as the velocity dropped through that of sound. Figs. 36 and 37 are from the analysis of a round fired before the war when both the measuring appliance and the methods of analysis were cruder. The accuracy of determination of velocity is to about 1 in 500. The shape and calibre of the projectile was different (6 J.R.H. instead of 7.5) and 1" instead of 20 mm but it is unlikely that the differences vitiate the comparison. It will be seen that the motion (for $M \approx 1.01$) is very similar. The remaining figures (38-45) of the same pre-war vintage tell a totally different story. Over the range covered ($0.75 < M < 0.9$) the motion is unstable. The basic or precessional component of the yaw increases considerably, the subsidiary or nutational component is constant or slightly damped.

The result that spin stabilized bodies of revolution (at any rate of projectile form) are unstable in the lower end of the transonic region is one that has been found in all firings carried out in the N.P.L. Ballistic Range. A detailed analytical quantitative explanation cannot be given at present but a qualitative explanation which is at least plausible can be given on the following lines. It is based on the fact that the "lift" of a projectile is provided by the head only and is small anyway.

The shock stall or lower critical Mach number for a projectile head is a function of its shape and yaw, typical values are $M_c = 0.85$ for no yaw dropping to 0.75 for 10° yaw, so that a projectile in relative motion to an air stream at these Mach numbers and a little above would experience, if it were yawing, violent pressure oscillations in the neighbourhood of its head. At somewhat higher Mach numbers (say 0.95 and above) the shocks have moved on to the parallel portion where they are relatively harmless since the pressure distribution here is symmetrical and boundary layer breakaway is fixed at the tail and is unlikely to move forward at these angles of yaw.

Fin stabilized bodies have never been fired in the range and it is therefore impossible to make any estimates of body-fin interaction in the transonic region, nor of the effect of fins in altering the range of the region of instability.

The oscillatory motion of the projectile is of course relative to its centre of gravity which is about two thirds of its length from the nose. Therefore insofar as comparison with aerofoils is valid the results correspond to an aerofoil oscillating about a pivot line about $2/3$ chord from the nose.

(b) The Unsteady State

With regard to the unsteady state (Gardner and Ludloff 1950) state that acceleration terms are only important when

$$\mathcal{M} < 1 + (2 \ddot{x} l / U^2)^{1/2}$$

where \ddot{x} is the deceleration.

In this case $\ddot{x} \approx 300$, $l \approx 1/3$, $U^2 \approx 1,000$ and the effect is only important for $\mathcal{M} < 1.01$. Phythian (1952) states a criterion in the form "the proportional change, while the body travels its own length, in linear or angular velocity must be small if the additional aerodynamic force coefficients induced by the change are to be small also". This criterion is satisfied in these firings. Unfortunately both these criteria are based on linearized theory and their accuracy near $\mathcal{M} = 1$ is, at least, open to question.

The direct analytical attack on the problem leads via von Kármán's transonic approximation to an equation which can be written

$$F_{\eta\eta} + \frac{1}{\eta} F_{\eta} = 2 F_{\xi} F_{\xi\xi} + A$$

with appropriate boundary conditions. A represents the acceleration terms which are constant in this case since the retardation is constant. This equation is non-linear in a very awkward way changing from hyperbolic to elliptic within the region to be considered. Enquiries of Mathematics Division, N.P.L. and elsewhere have revealed that the analytical theory of such equations is for practical purposes non-existent and that numerical solution would be very laborious and difficult. It does however seem likely that the presence of the A term would not appreciably increase the difficulties.

Lin, Reissner and Tsien (1948) have carried the discussion a little further and reach the conclusion that the problem is quasi steady if

$$K \ll \delta^{2/3}$$

wherein $\delta \equiv$ thickness ratio

and $K \equiv \omega b/U$ (the frequency parameter).

Here $\delta \approx 0.2$ since the projectiles are about 5 calcs. long and

$$K \approx \frac{2\pi \times 40 \times 1/3}{1000} \approx 0.08 \ll \delta^{2/3} (= 0.34)$$

so that the problem is quasi stationary by their criterion.

Therefore though the correction cannot be evaluated it seems reasonably certain that the oscillatory motion of the projectile has not affected the numerical results, but that the retardation may have had an effect very near $\mathcal{M} = 1$.

Finally the first ten figures and Fig. 31 have a topical interest in connection with sonic bangs and could with advantage be studied in conjunction with (for instance) the figures of Lilley et al (1953).

Acknowledgements/

Acknowledgements

The rounds were fired and the analysis carried out by Messrs D. W. Bailey, D. A. Harding, E. G. Saunders and W. Watson, members of the Ballistic Range Team of the Gas Dynamics group of the erstwhile Engineering Division, N.P.L.

REFERENCES

<u>No.</u>	<u>Author(s)</u>	<u>Title, etc.</u>
1	Gardner Ludloff	Influence of acceleration on aerodynamic characteristics of thin aerofoils in supersonic and transonic flight. Journ. Ae. Sci. 1950, 17, 47.
2	J. E. Fythian	Some unsteady motions of a slender body through an inviscid gas. Q.Journ.Mech. & App. Math. 1952, V. 301.
3	C. C. Lin E. Reissner H. S. Tsien	On two dimensional non-steady motion of a slender body in a compressible fluid. Journ. Math. & Phy. 1948, 27, 220.
4	G. M. Lilley R. Westley A. H. Yates J. R. Busing	Some aspects of noise from supersonic aircraft. Journ. R.Ae.S. 1953, 57, 396.
5	-	Modern developments in fluid dynamics. High Speed Flow, Volume II. O.U.P. 1953.

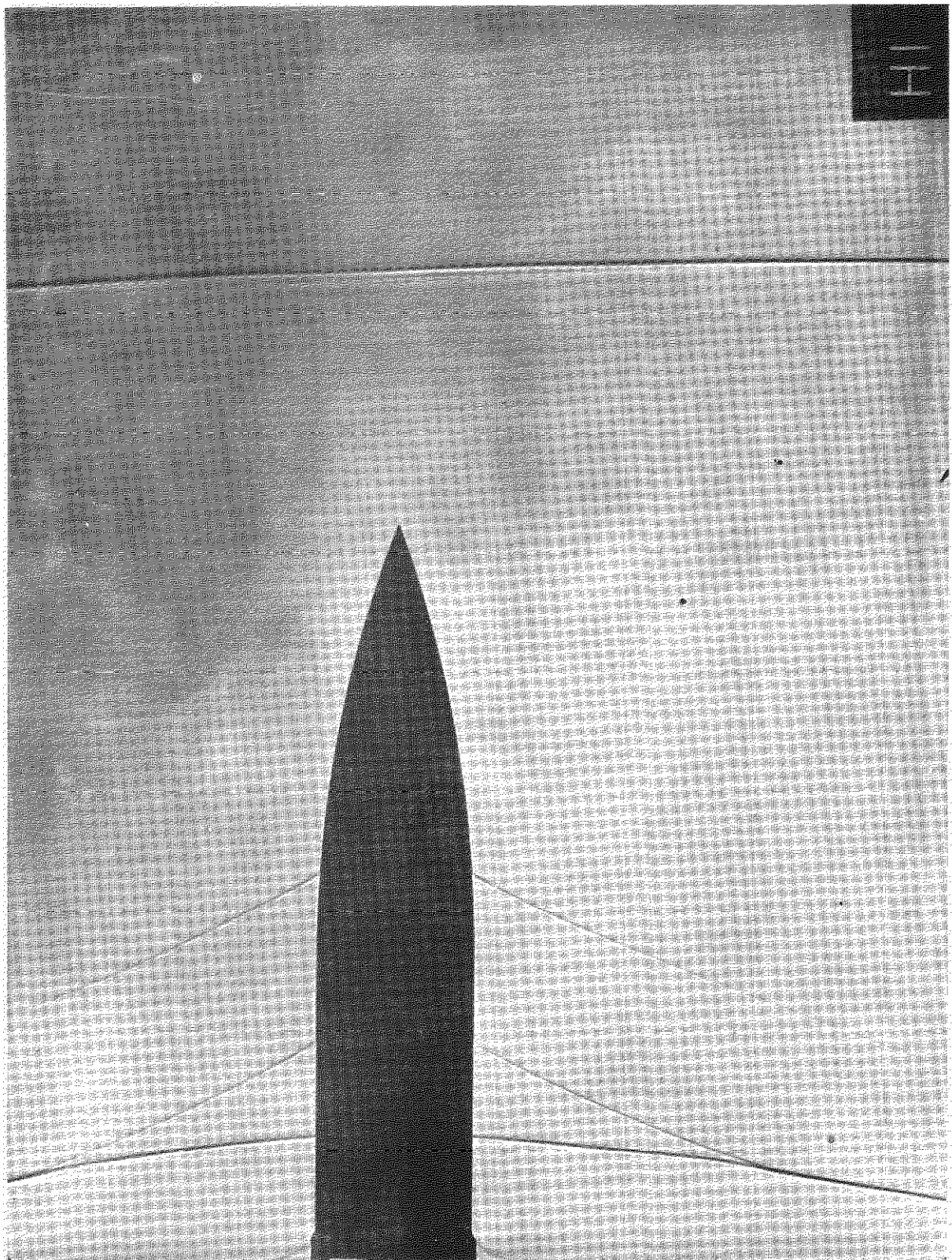


Fig. 1: Projectile F117, 1136 f.s., $M = 1.009$



Fig. 2: Projectile F117, 1128 f.s., $M = 1.002$



Fig. 3: Projectile M117, 1124 f.s., $M = 0.998$

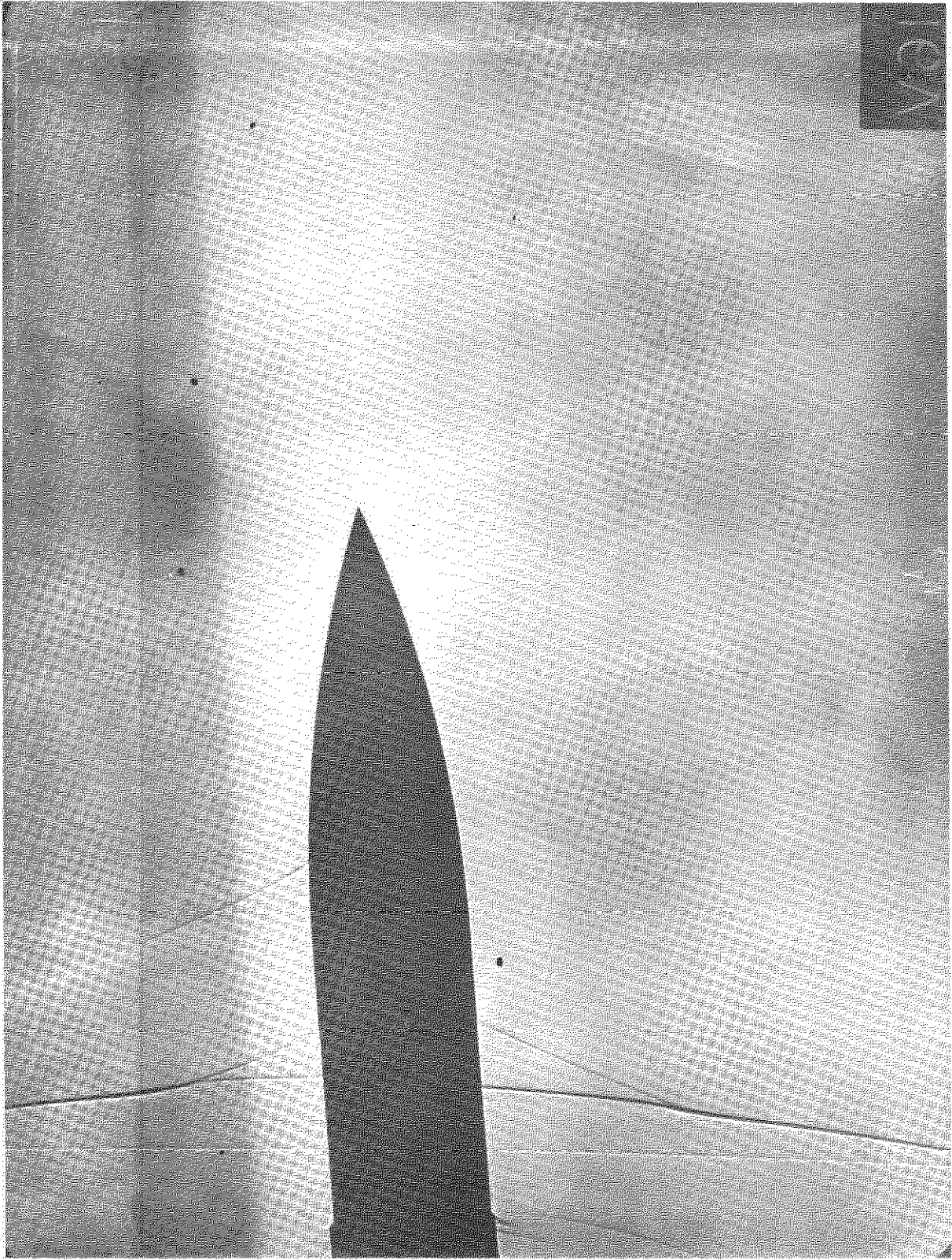


Fig. 4: Projectile F117, 1116 f.s., $M = 0.991$

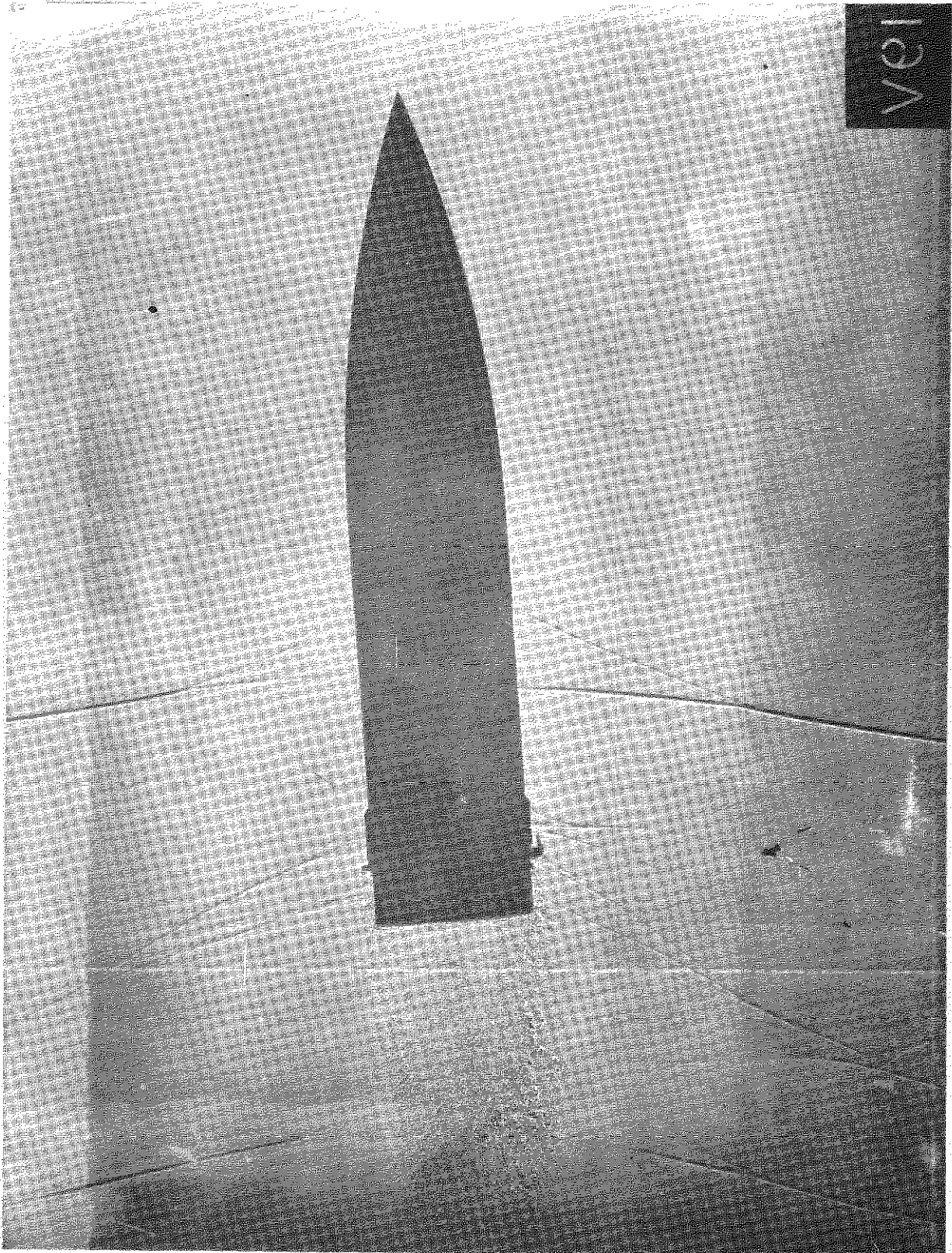


Fig. 5: Projectile F117, 1113 f.s., $M = 0.988$

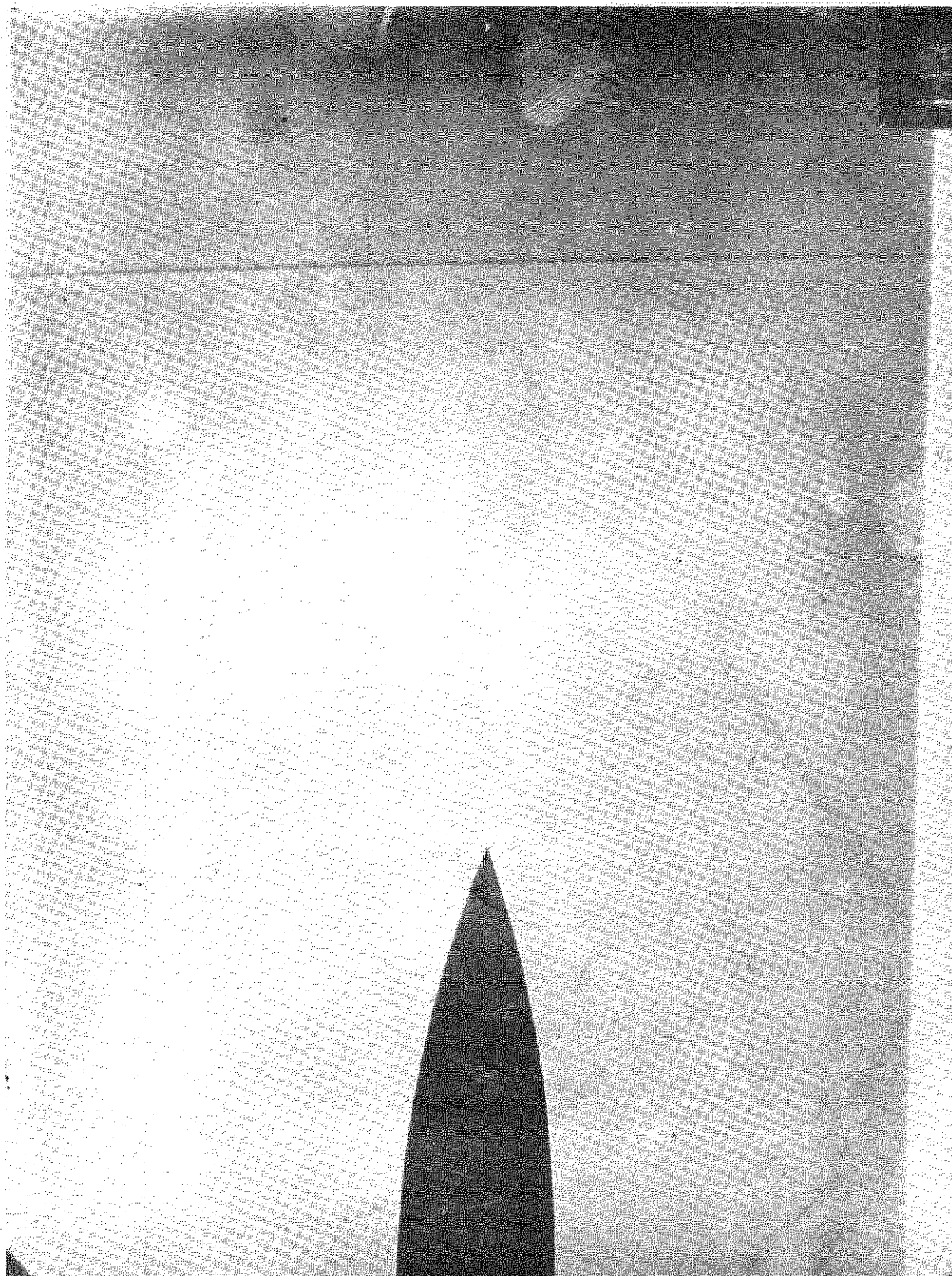


Fig. 6: Projectile F121, 1123 f.s., $M = 1.000$

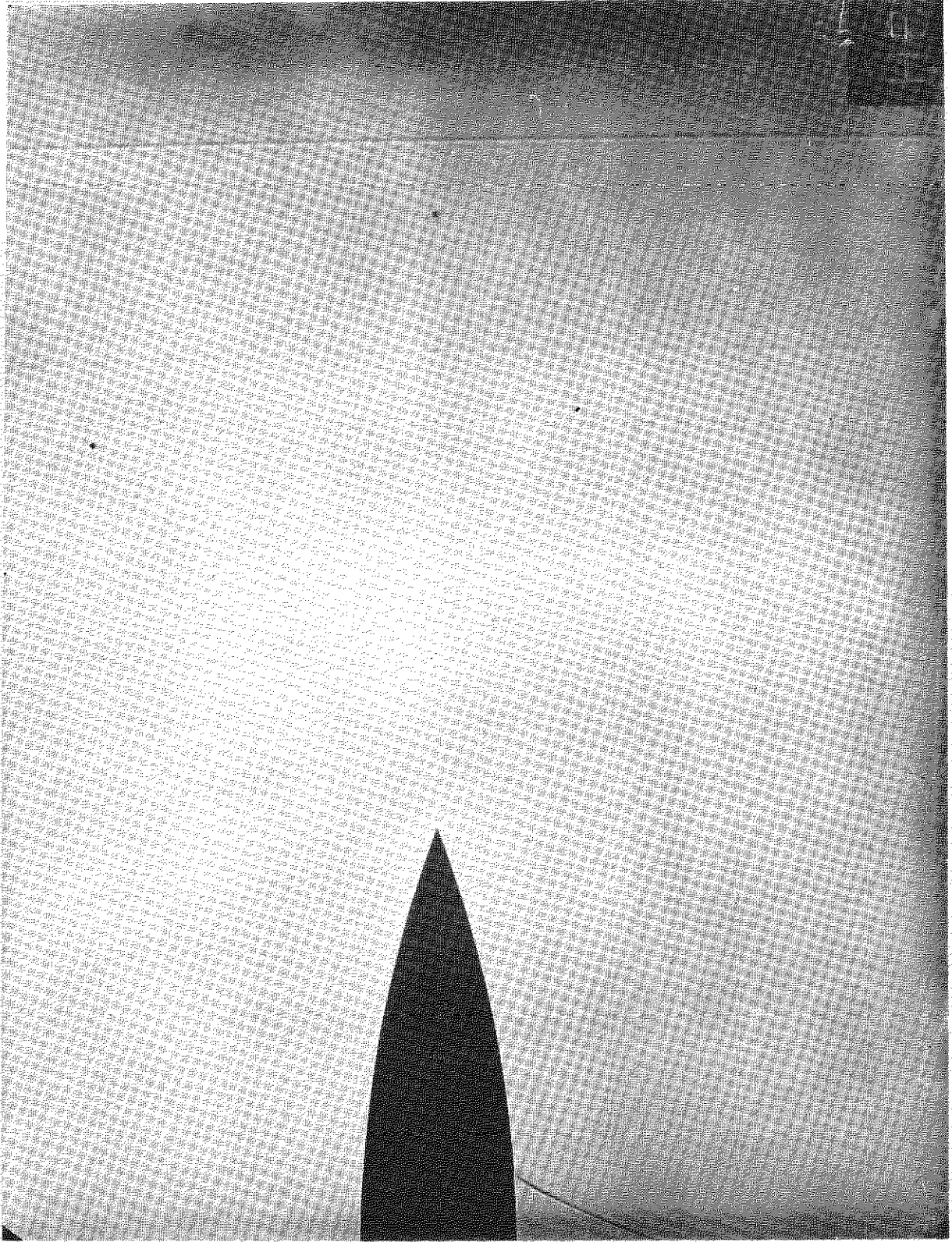


Fig. 7: Projectile F121, 1120 f.s., $M = 0.997$

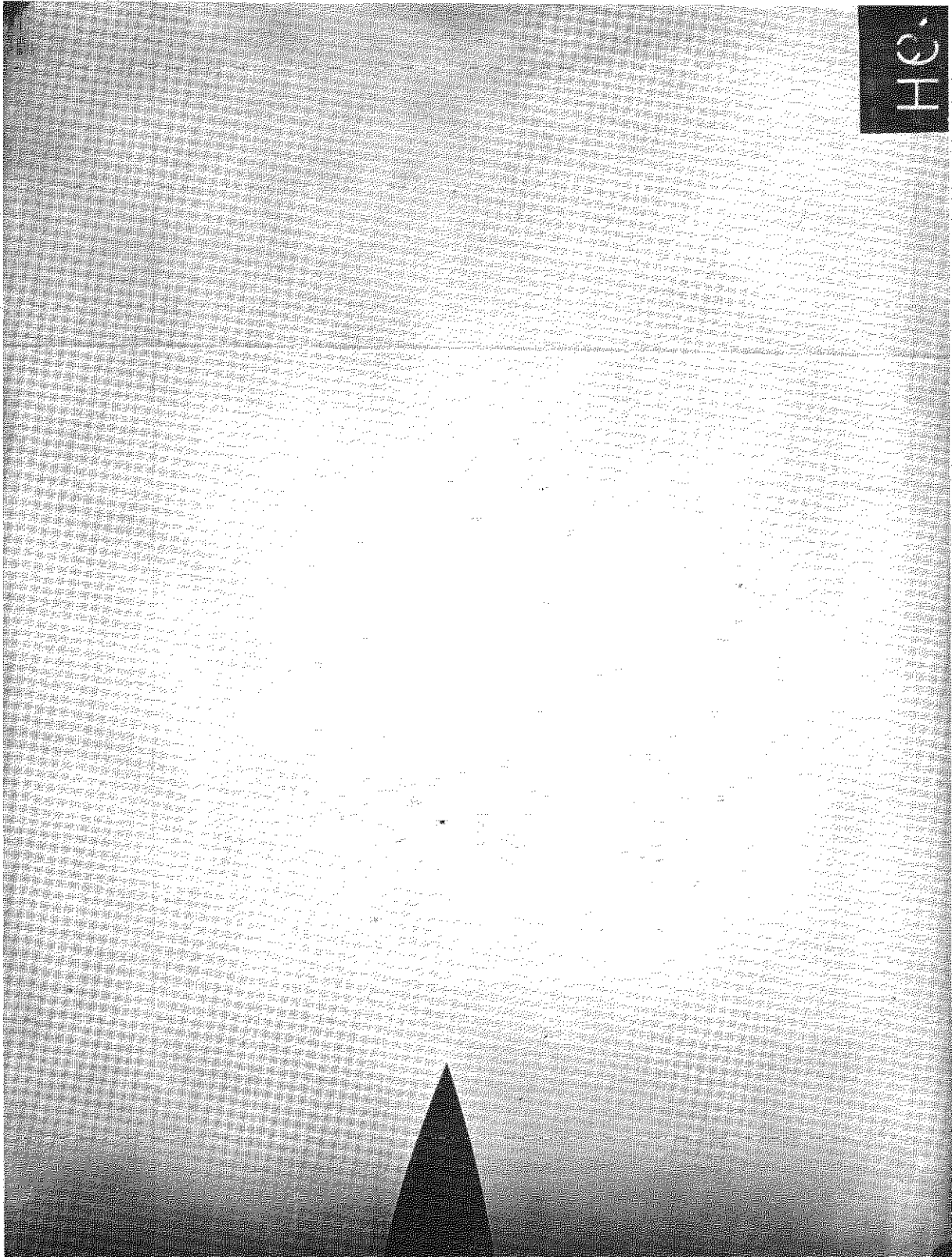


Fig. 8: Projectile P121, 1119 f.s., $M = 0.996$

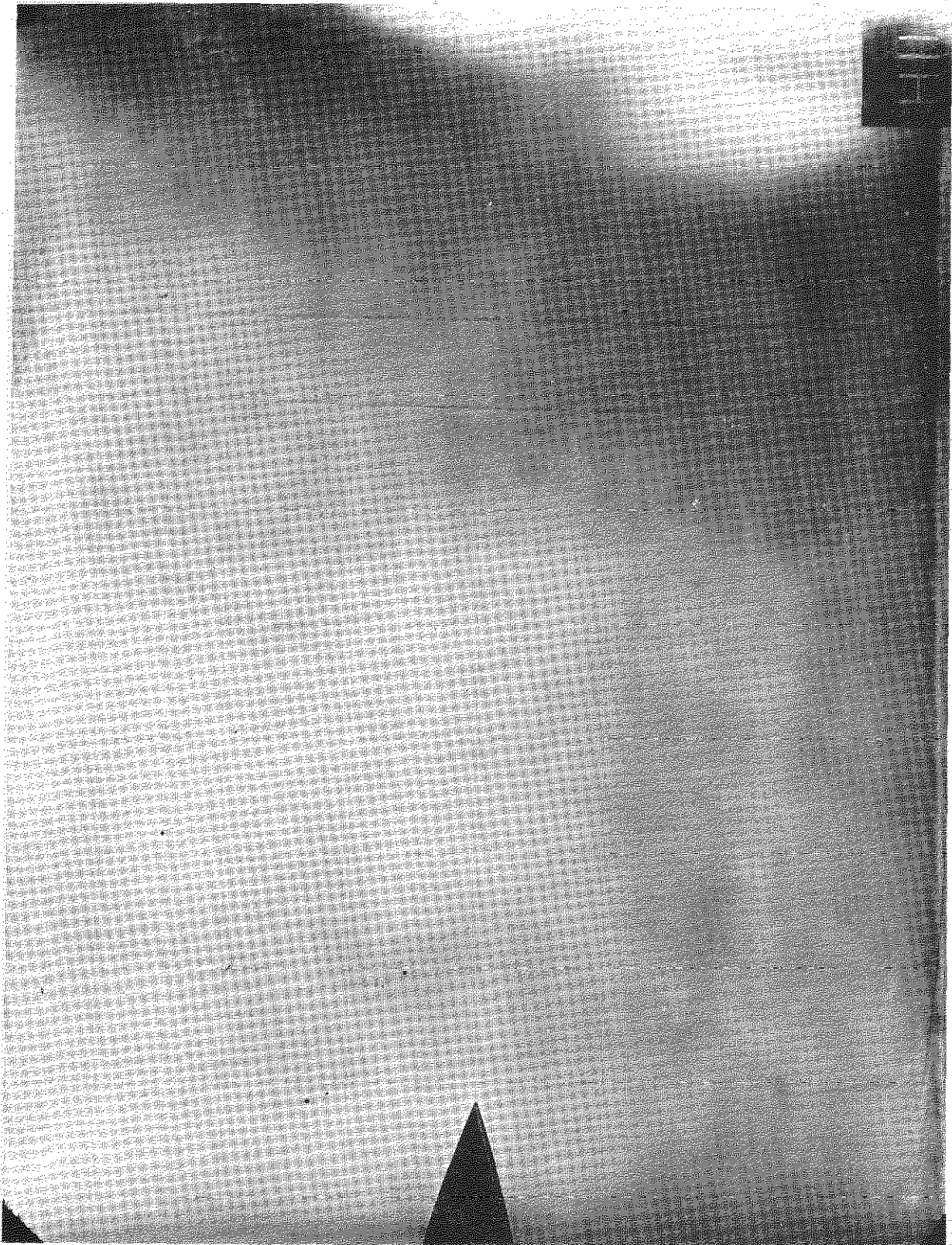


Fig. 9: Projectile F121, 1118 f.s., $M = 0.995$



Fig. 10: Projectile F121, 1118 f.s., $M = 0.995$

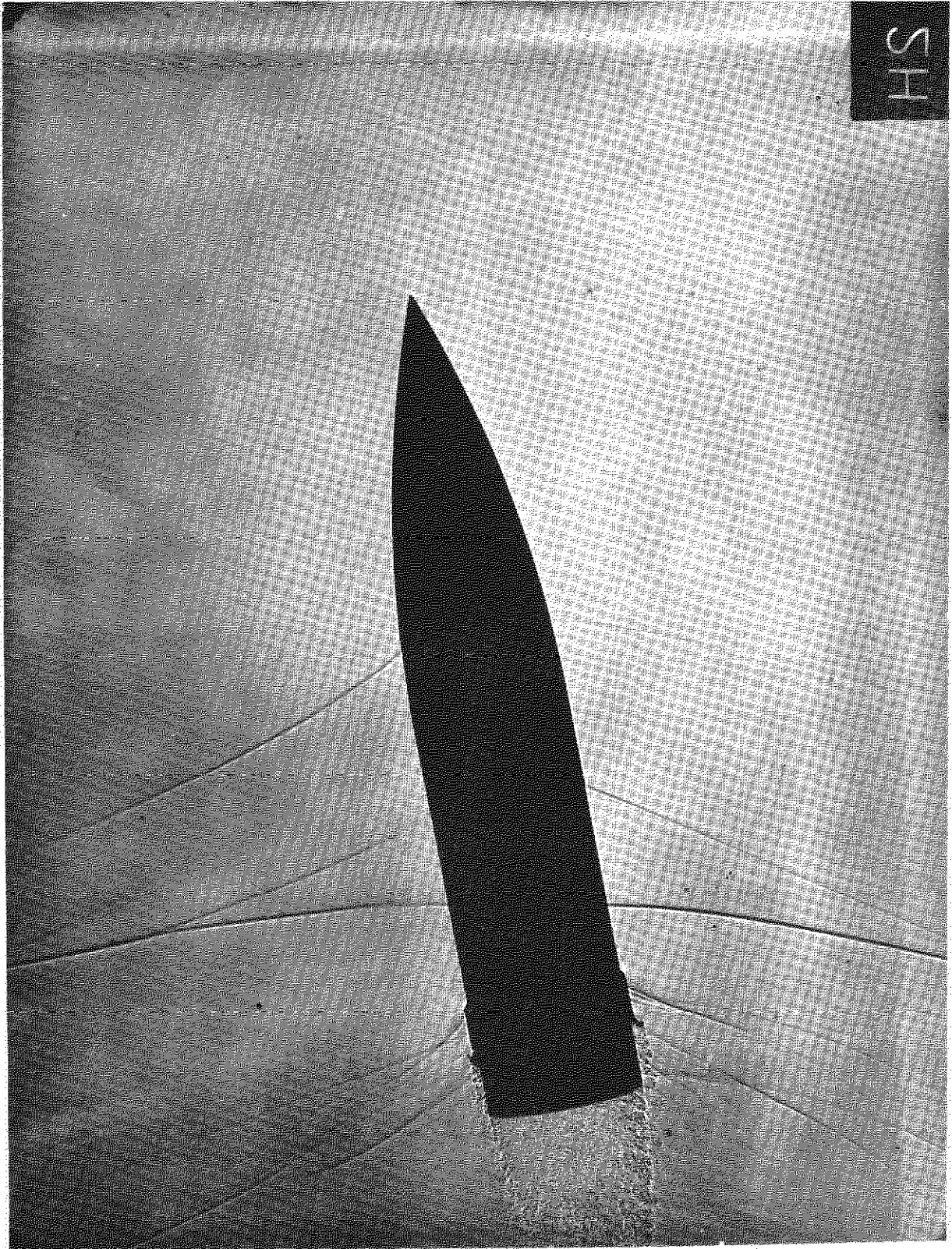


Fig. 11: Projectile F119, 1131 f.s., $M = 1.005$

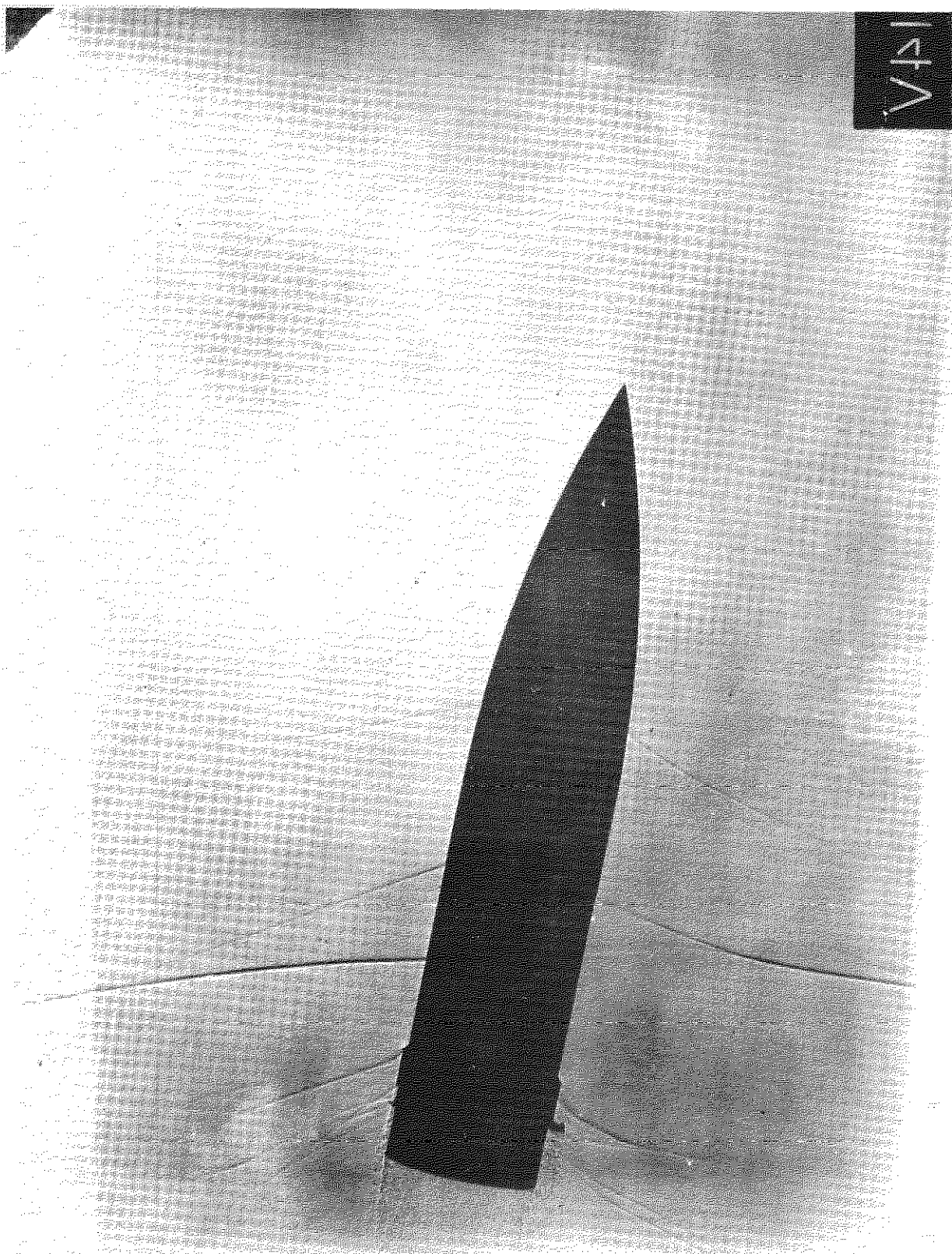


Fig. 12: Projectile F119, 1114 fs., $M = 0.990$

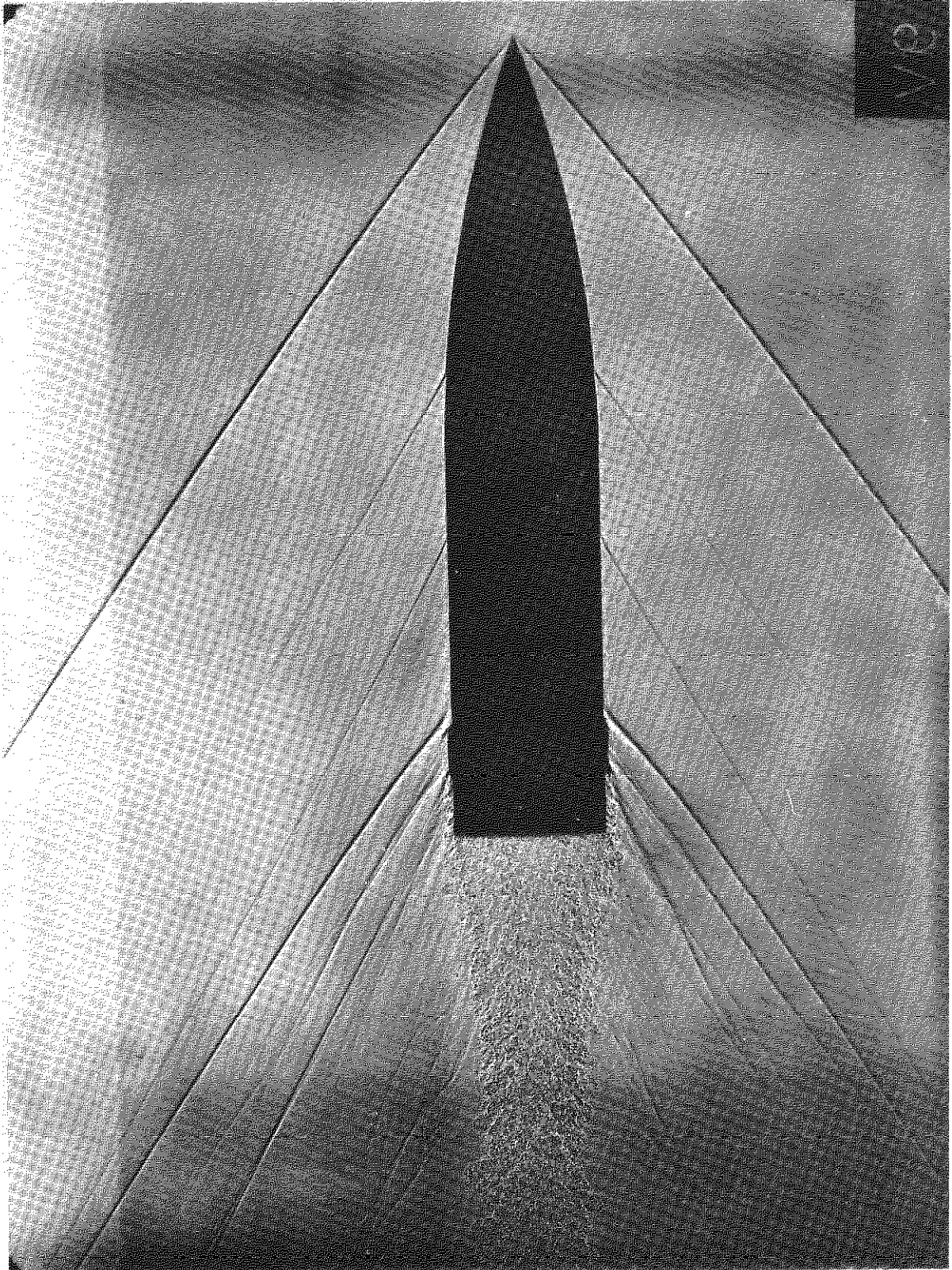


Fig. 13: Projectile F102, 2100 f.s., $M = 1.86$

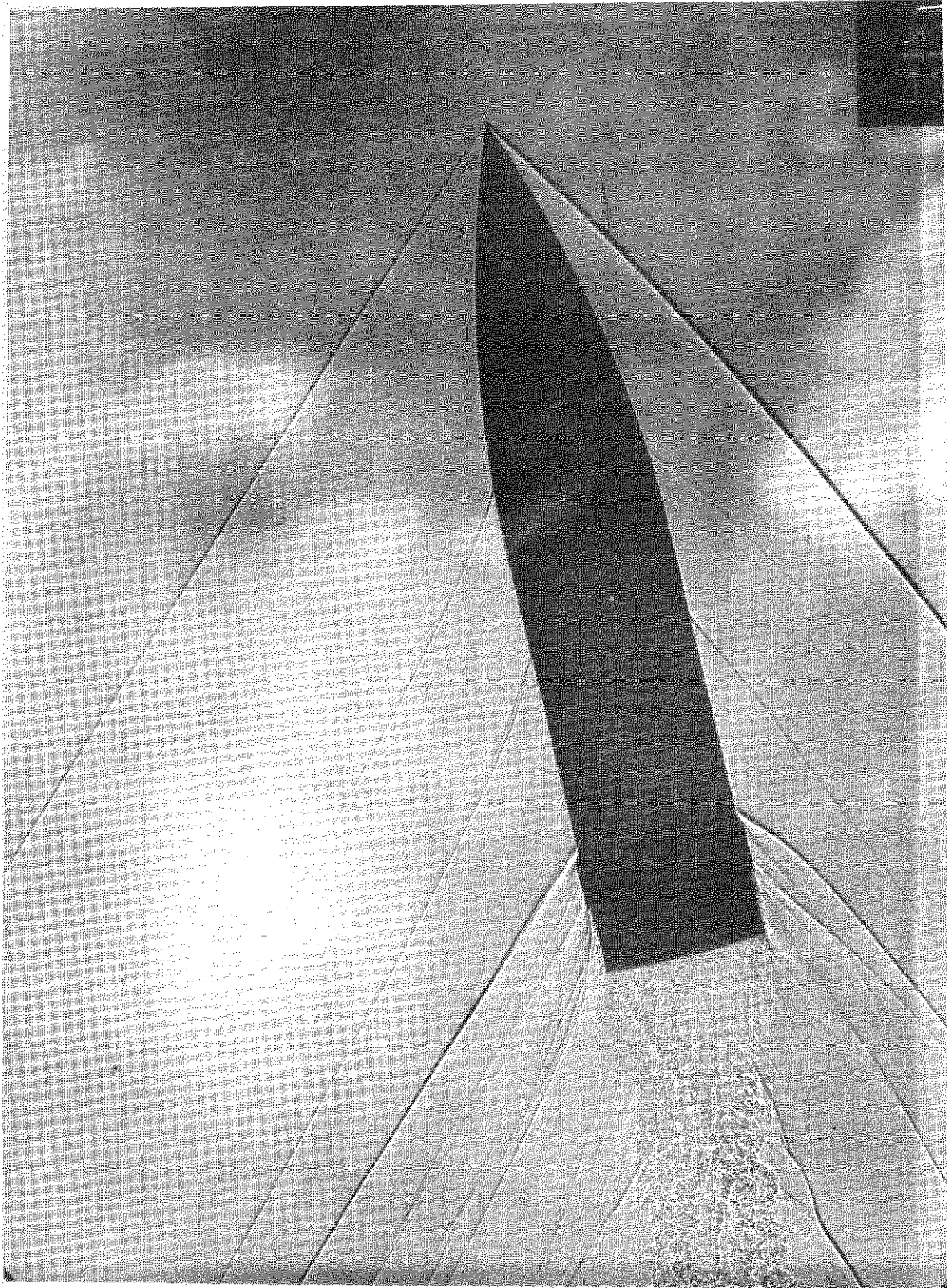


Fig. 14: Projectile F105, 2085 f.s., $M = 1.84$

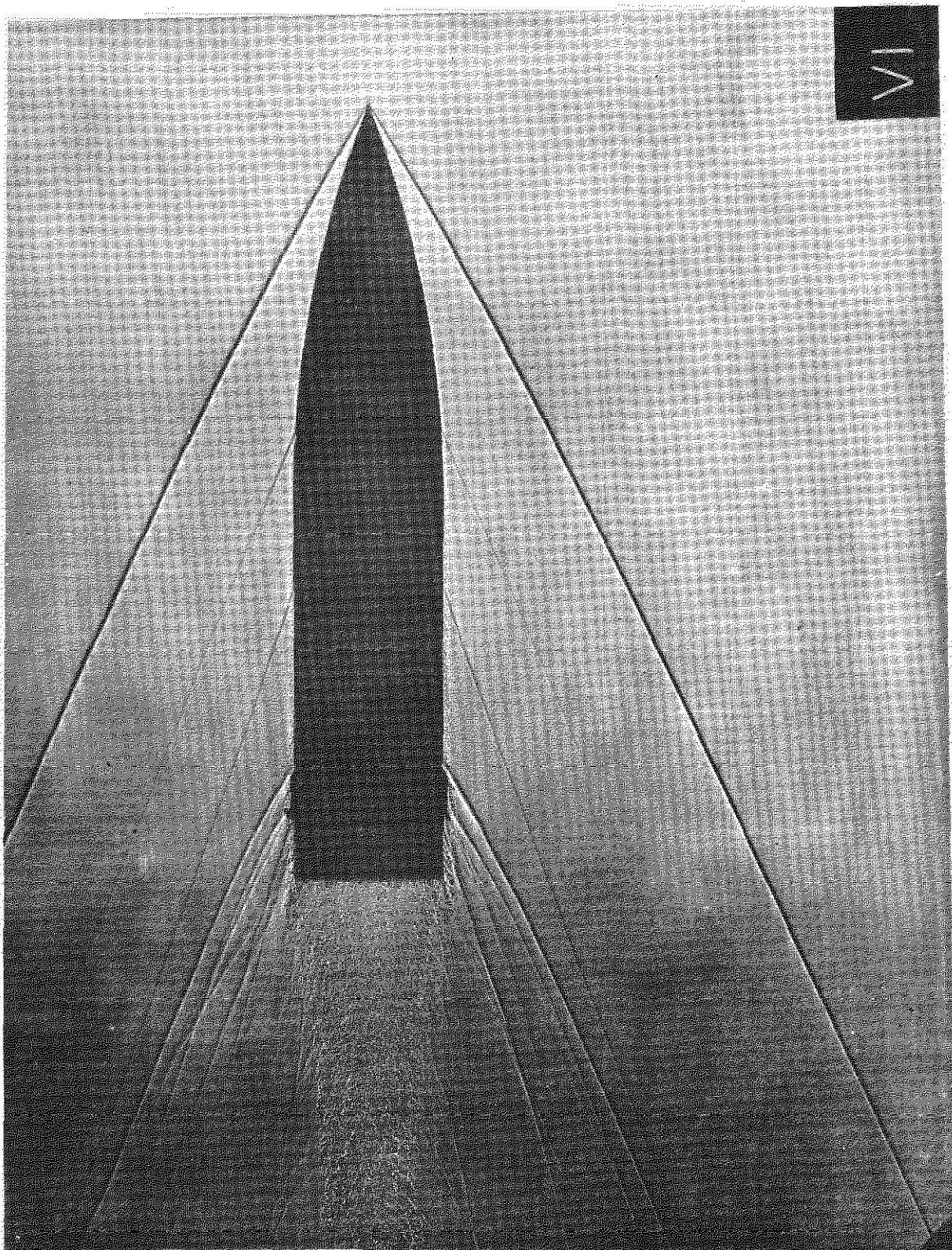


Fig. 15: Projectile F108, 3120 f.s., $M = 2.75$

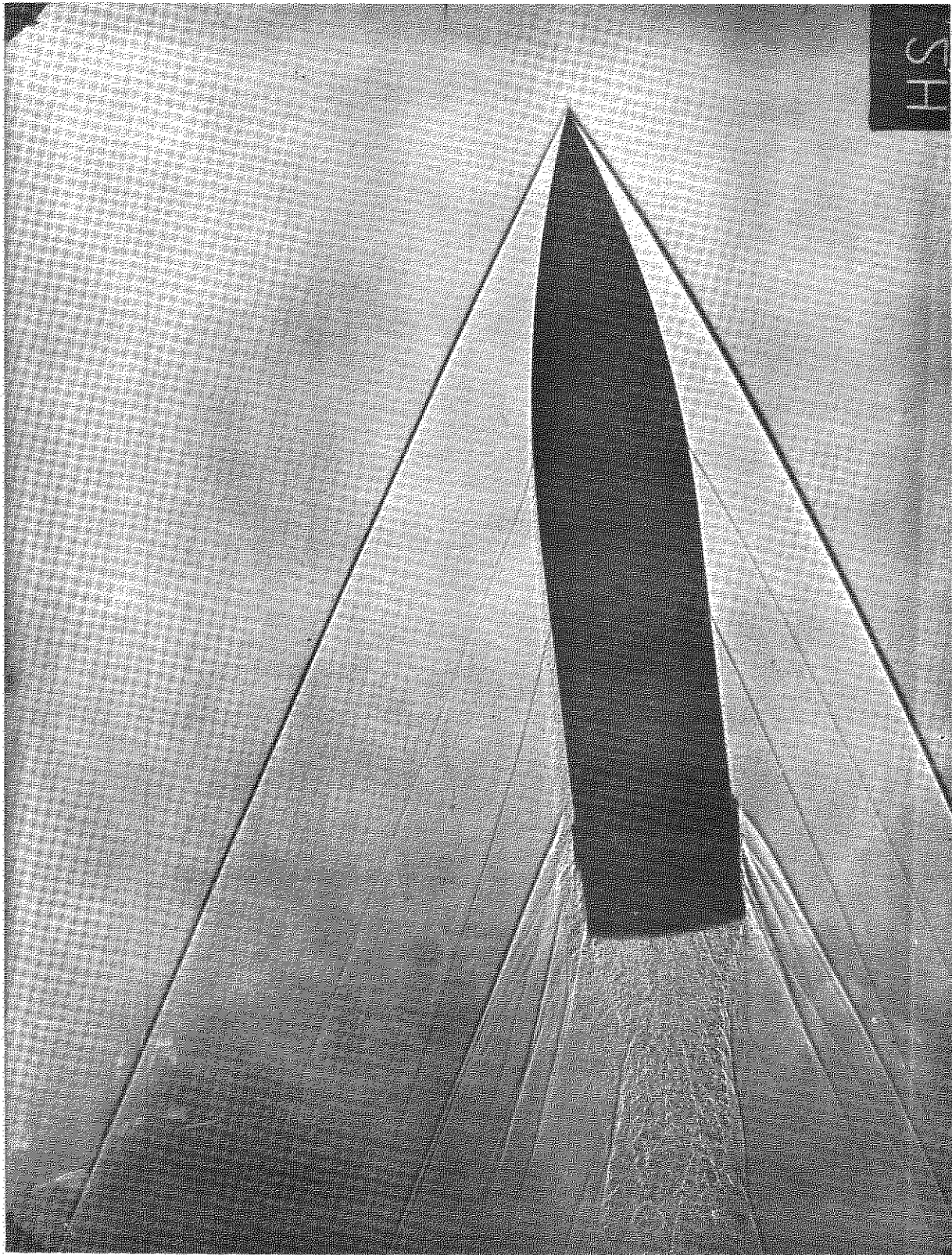


Fig. 16: Projectile F112, 3115 f.s., $M = 2.76$

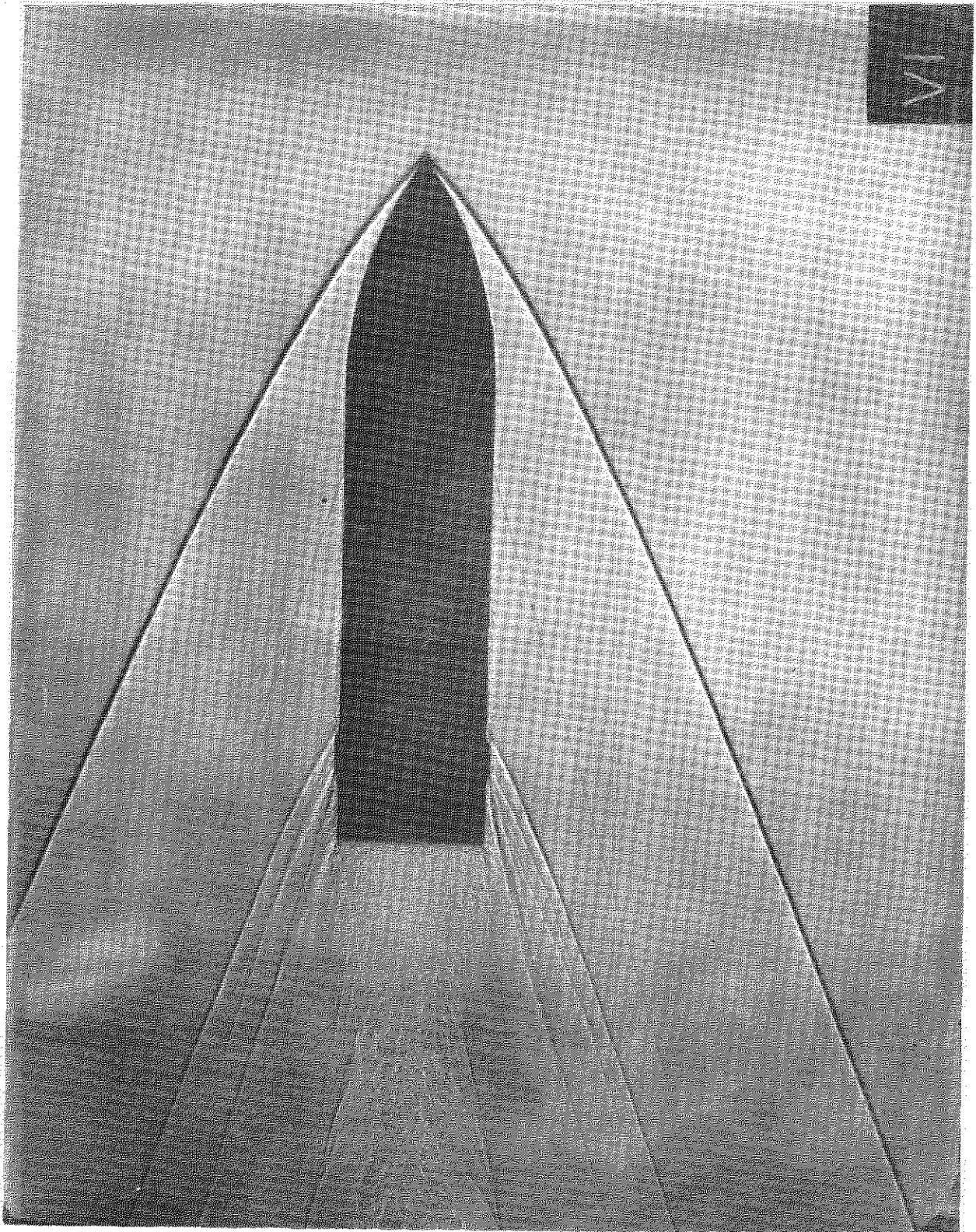


Fig. 17: Projectile I104, 3450 f.s., $M = 3.08$

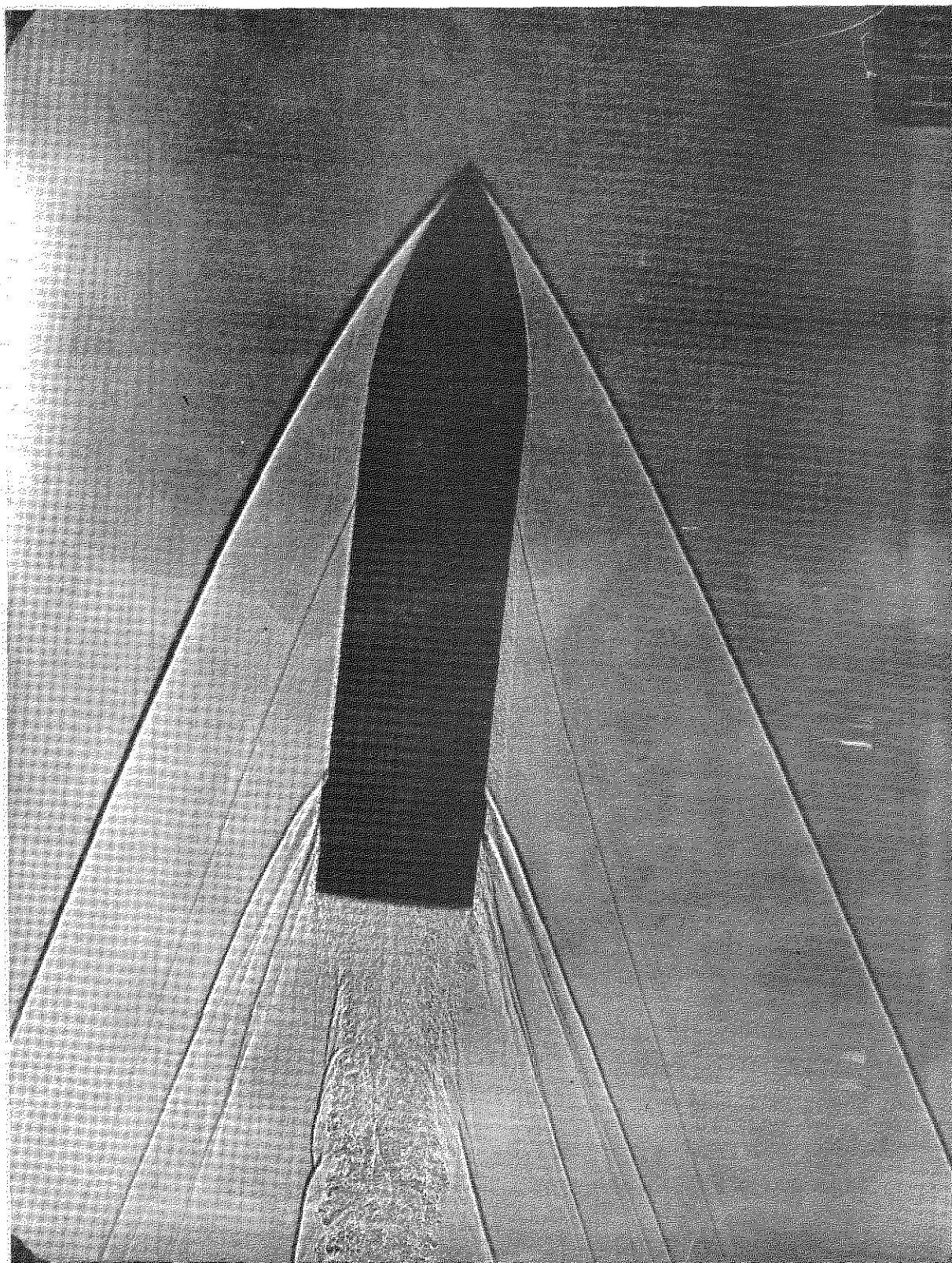


Fig. 18: Projectile I108, 3475 f.s., $M = 3.09$

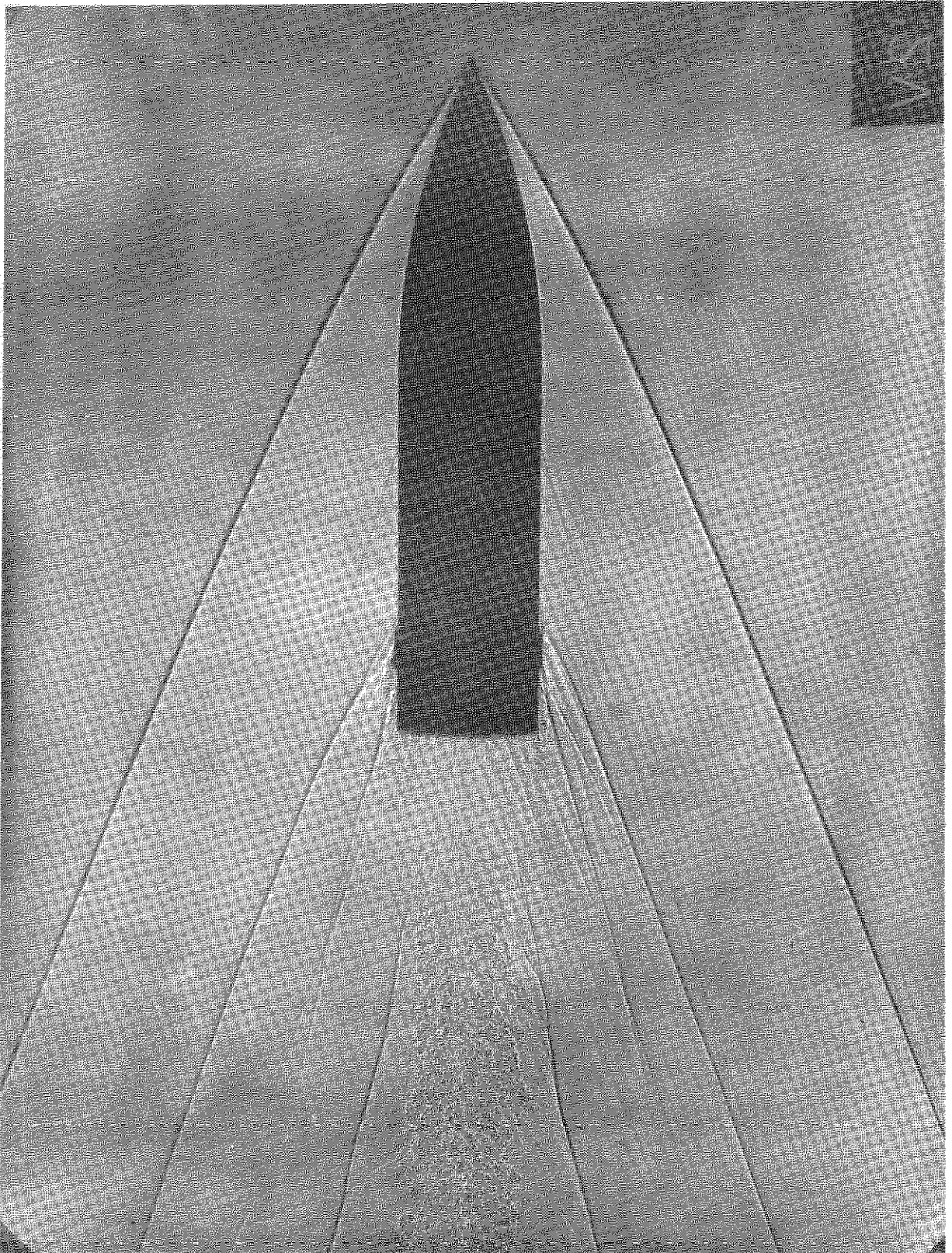


Fig. 19: Projectile E101, 3480 f.s., $M = 3.10$

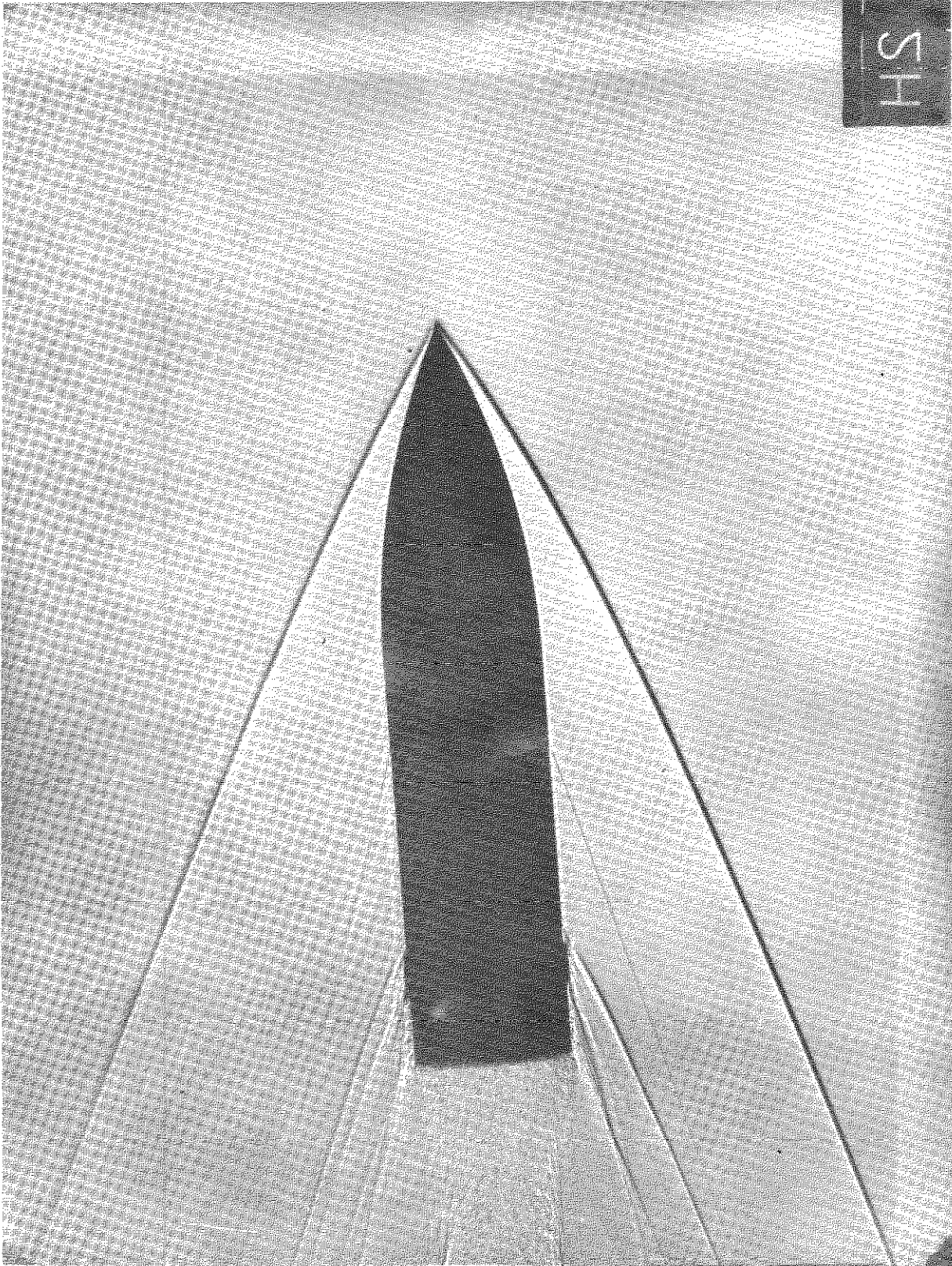


Fig. 20: Projectile E103, 3510 f.s., $M = 3.12$

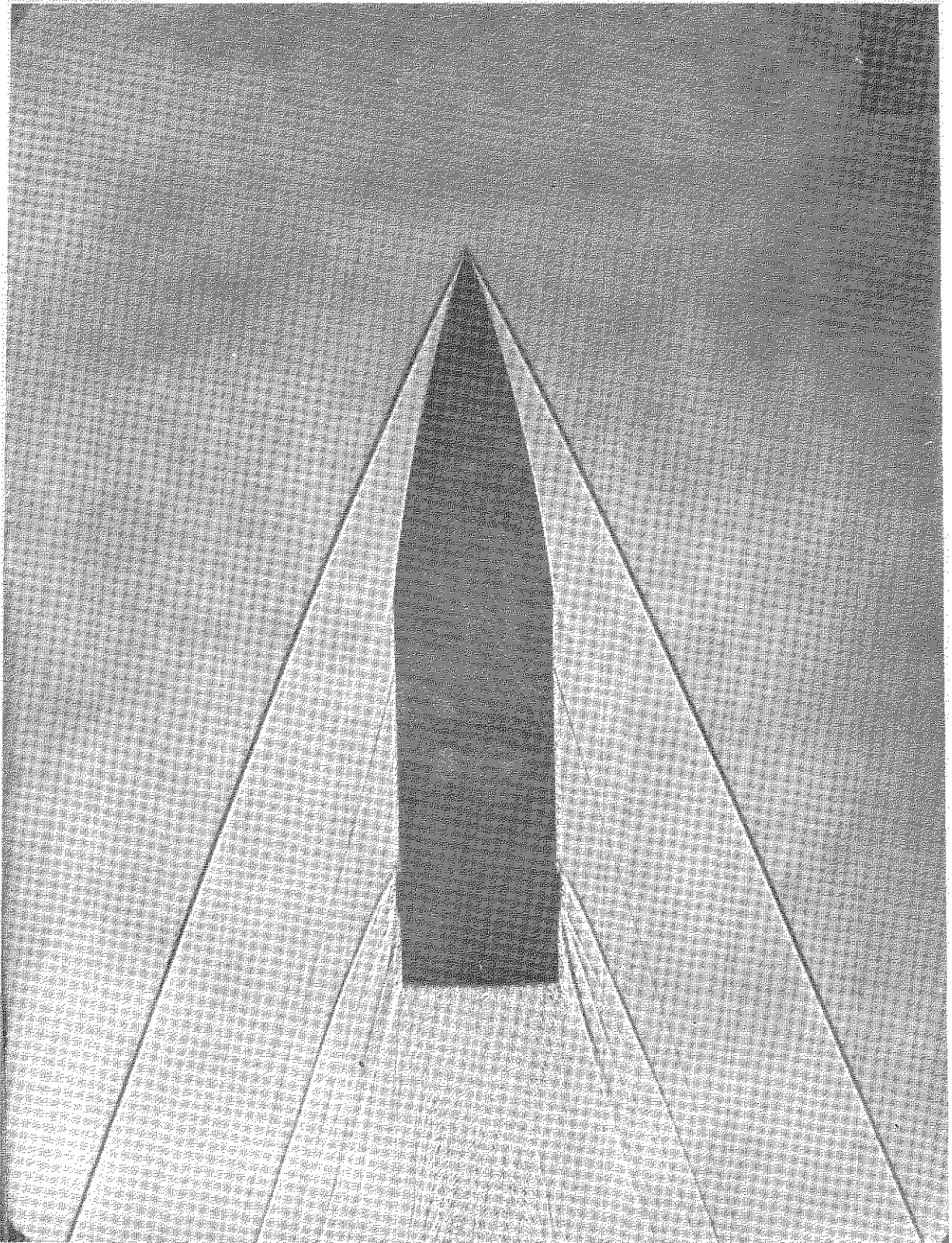


Fig. 21: Projectile 0100, 3495 f.s., $M = 3.10$

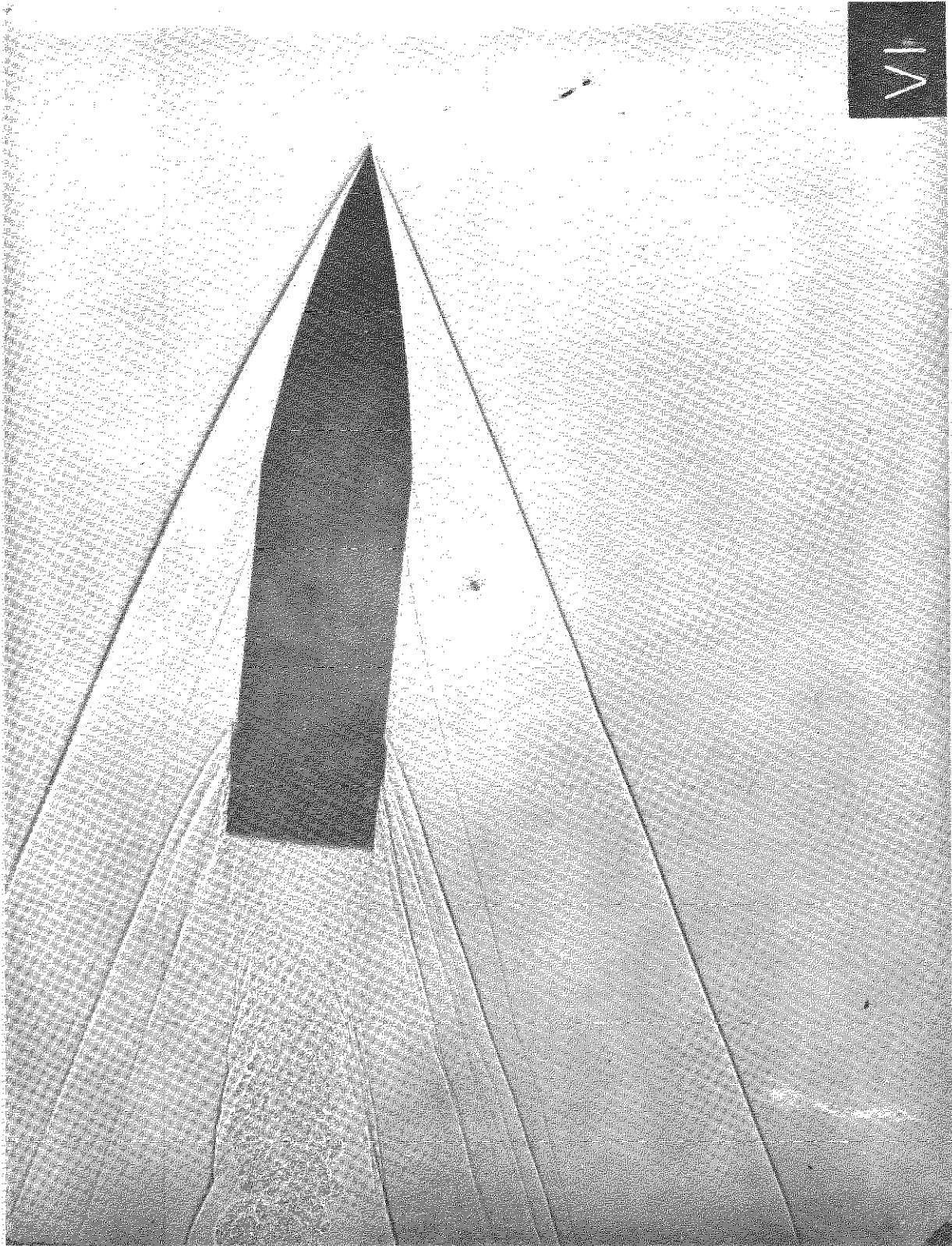


Fig. 22: Projectile 0103, 3510 f.s., $M = 3.12$

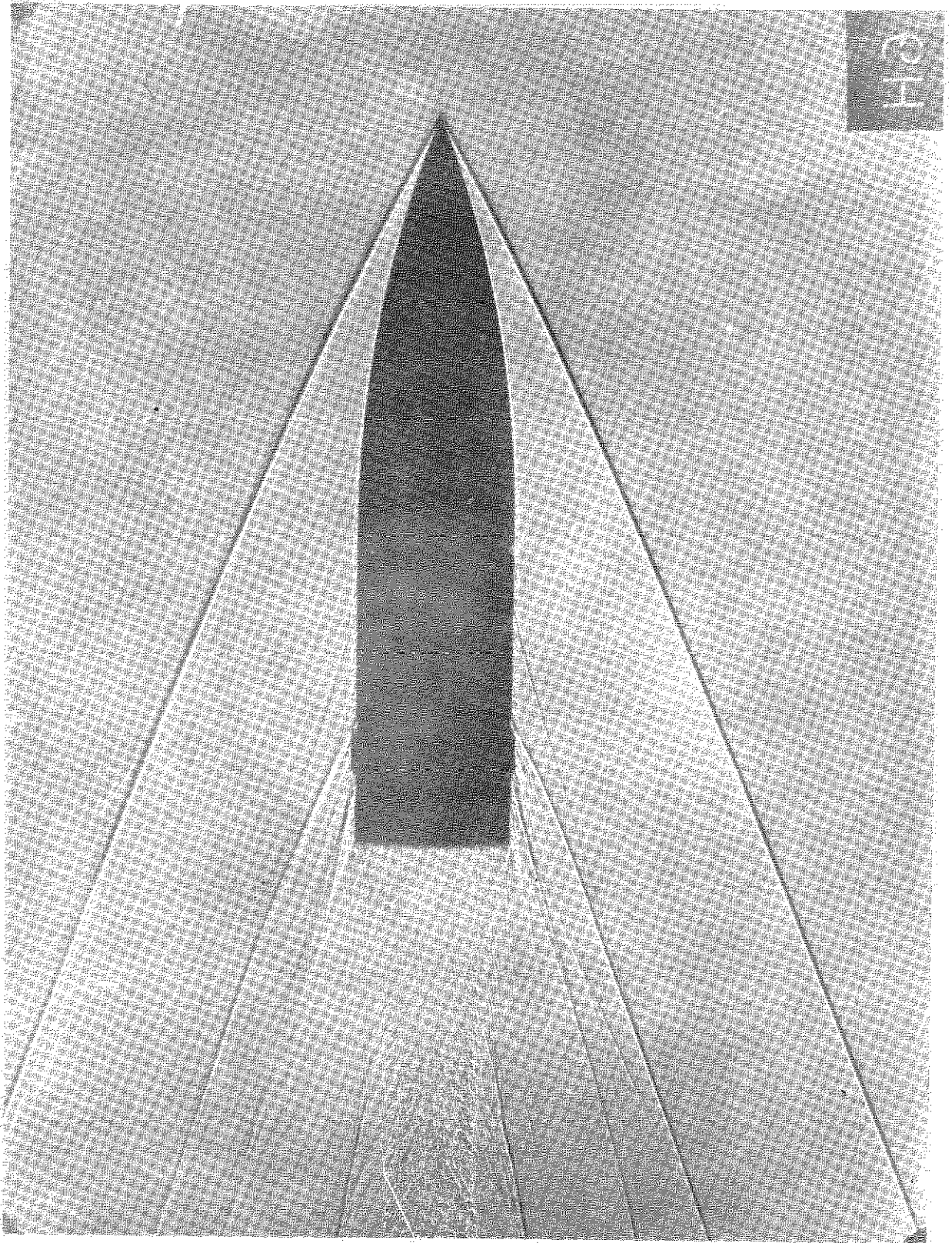


Fig. 23: Projectile 3A, 3505 f.s., $M = 3.11$

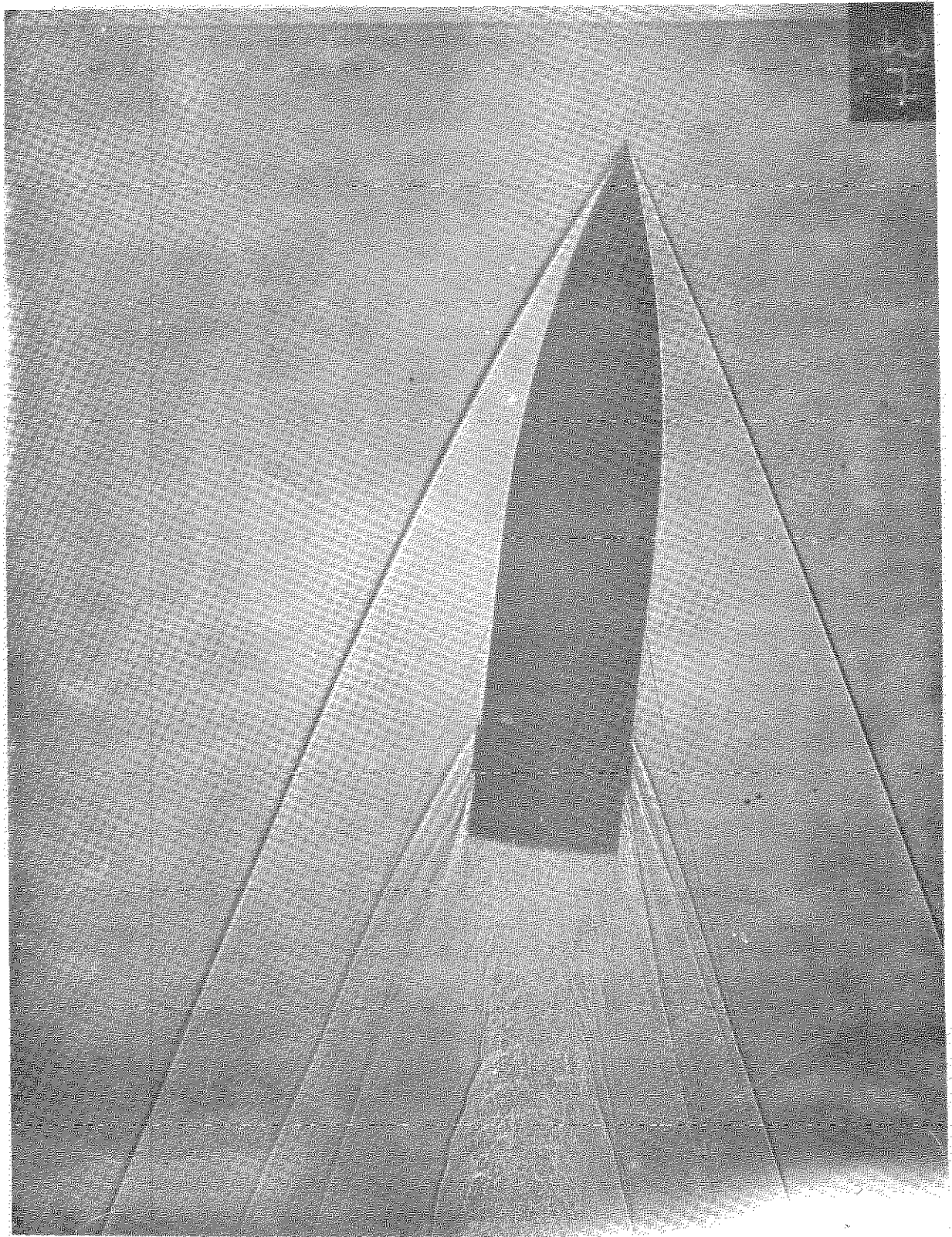


Fig. 24: Projectile 6A, 3500 f.s., $M = 3.10$

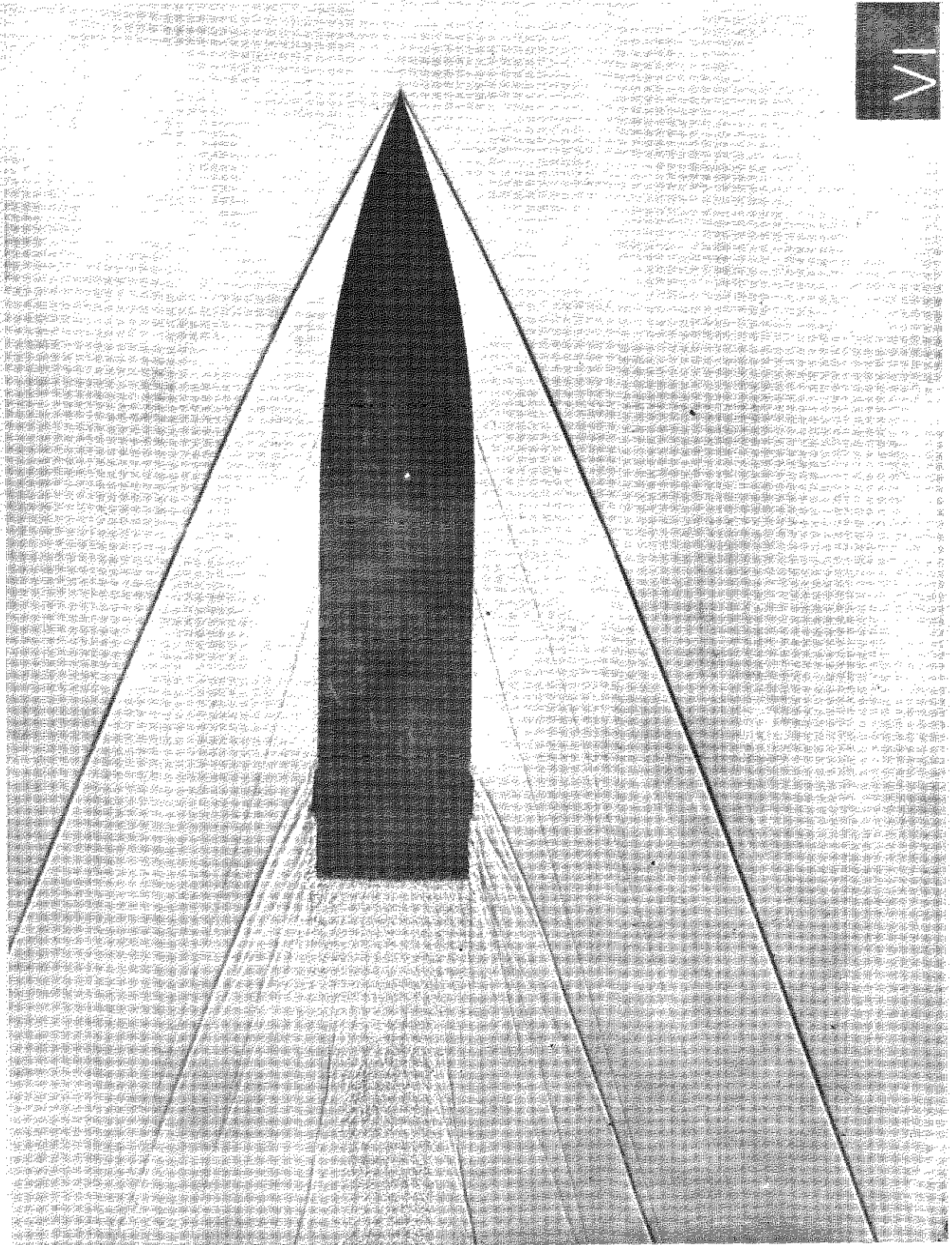


Fig. 25: Projectile F114, 3510 f.s., $M = 3.11$

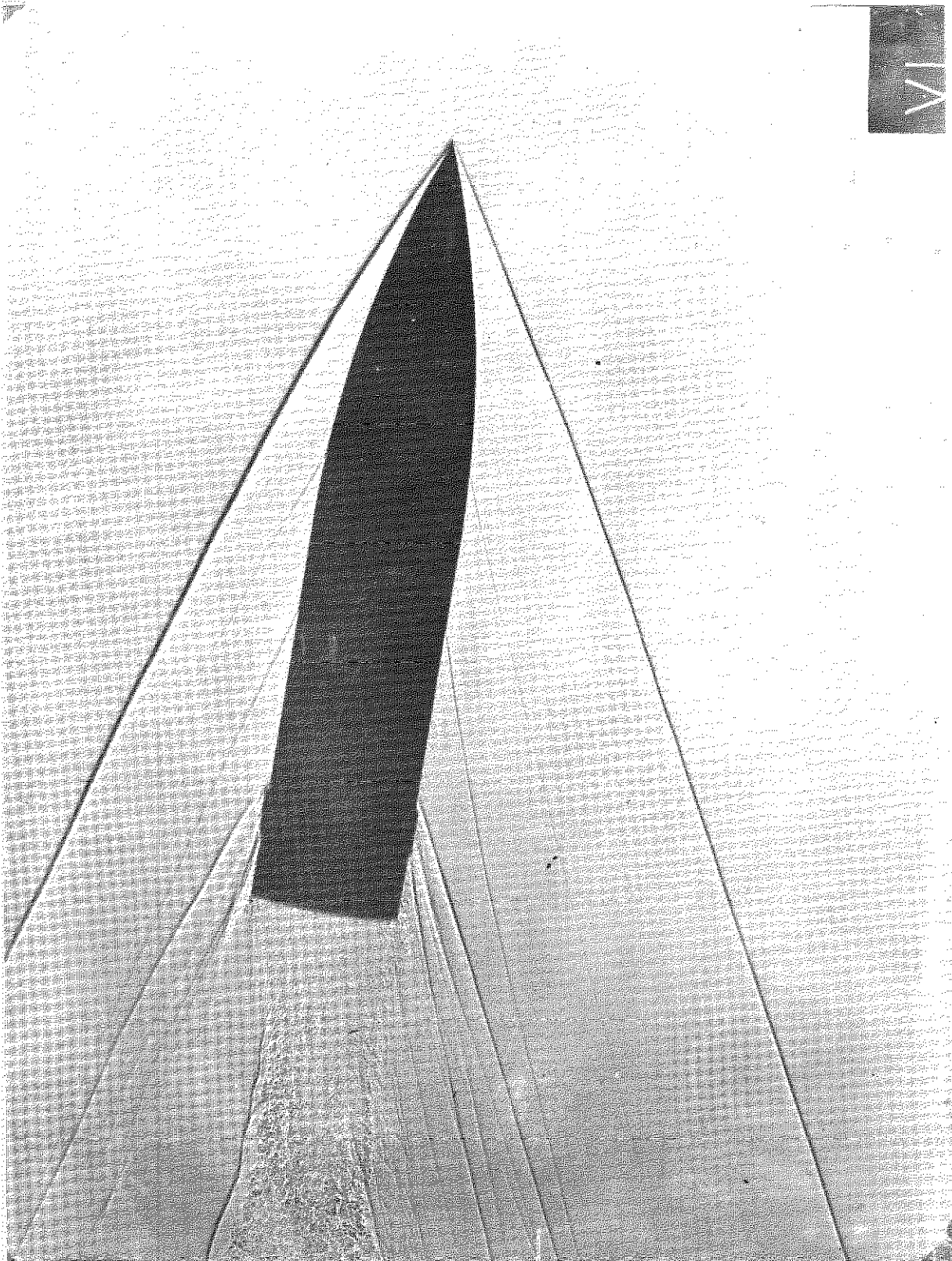


Fig. 26: Projectile F115, 3510 f.s., $M = 3.12$

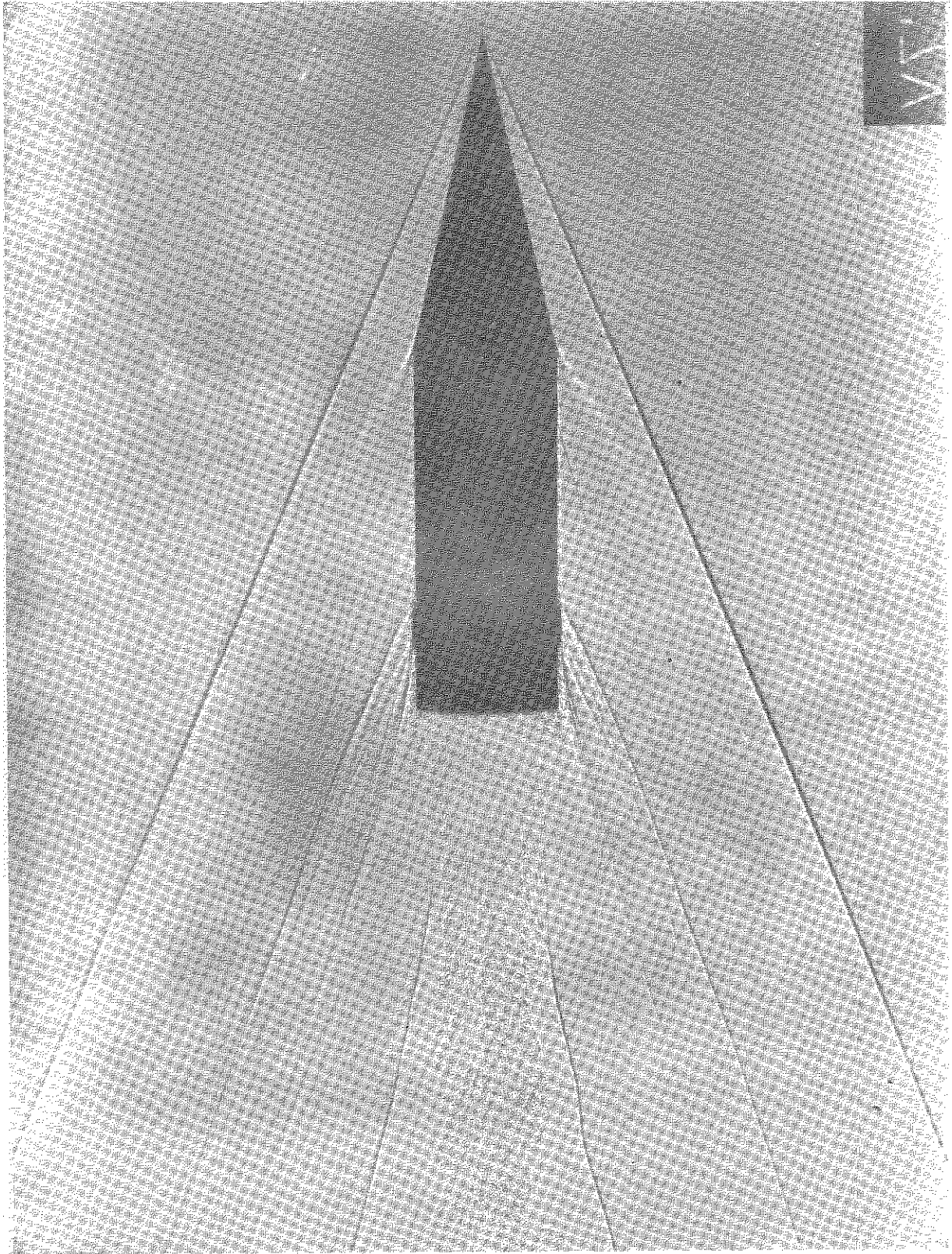


Fig. 27: Projectile N101, 3495 f.s., $M = 3.10$

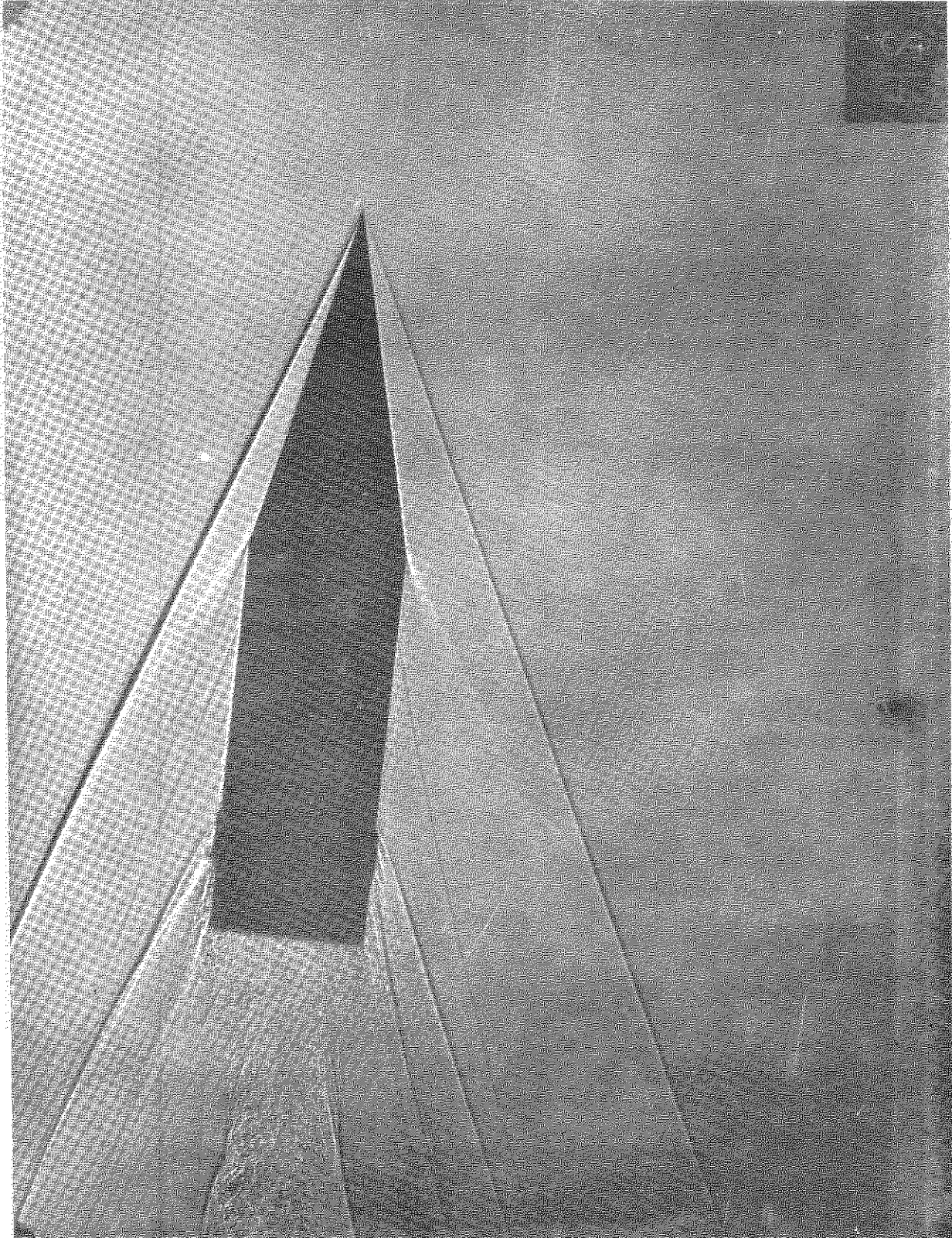
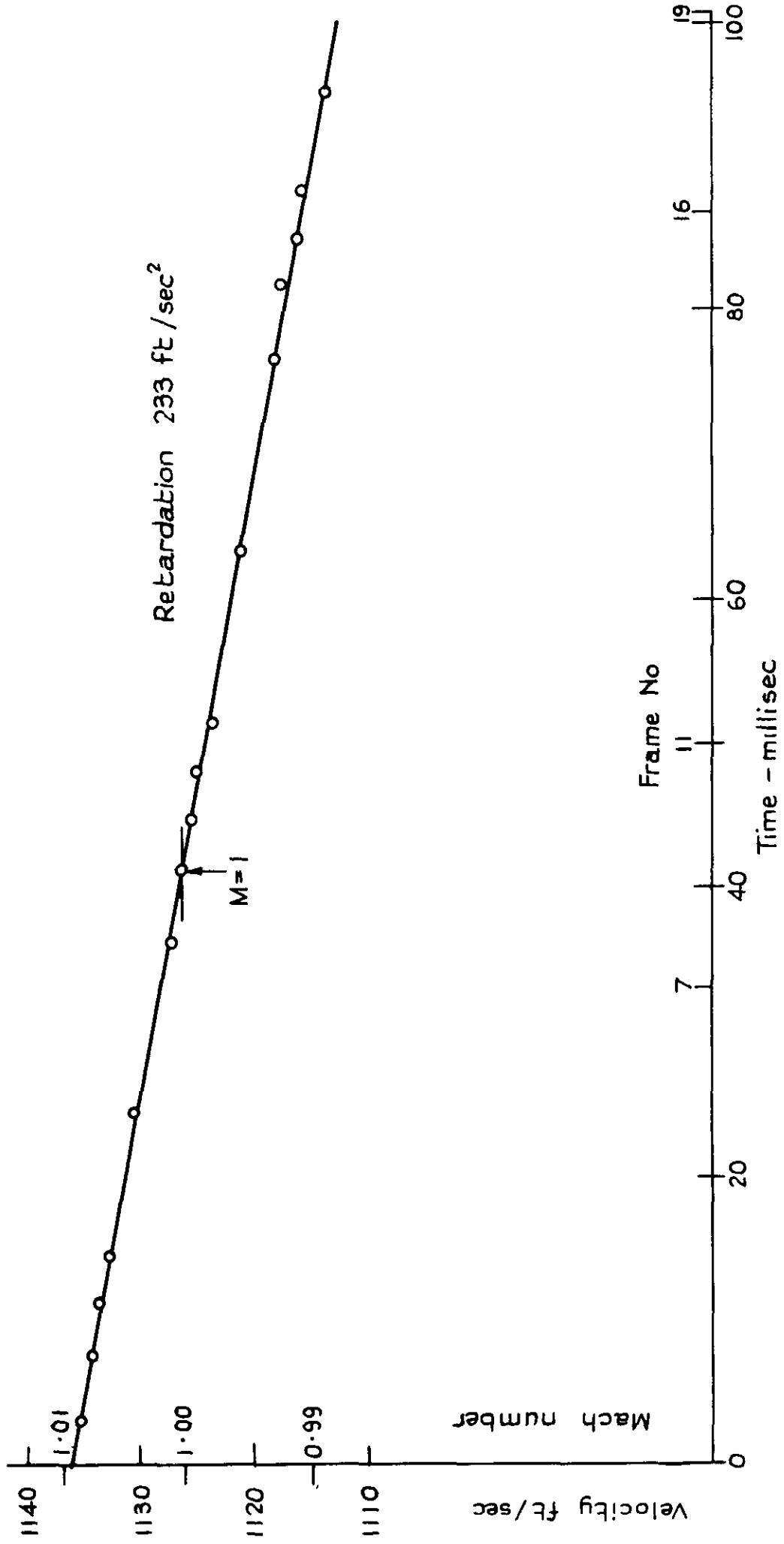


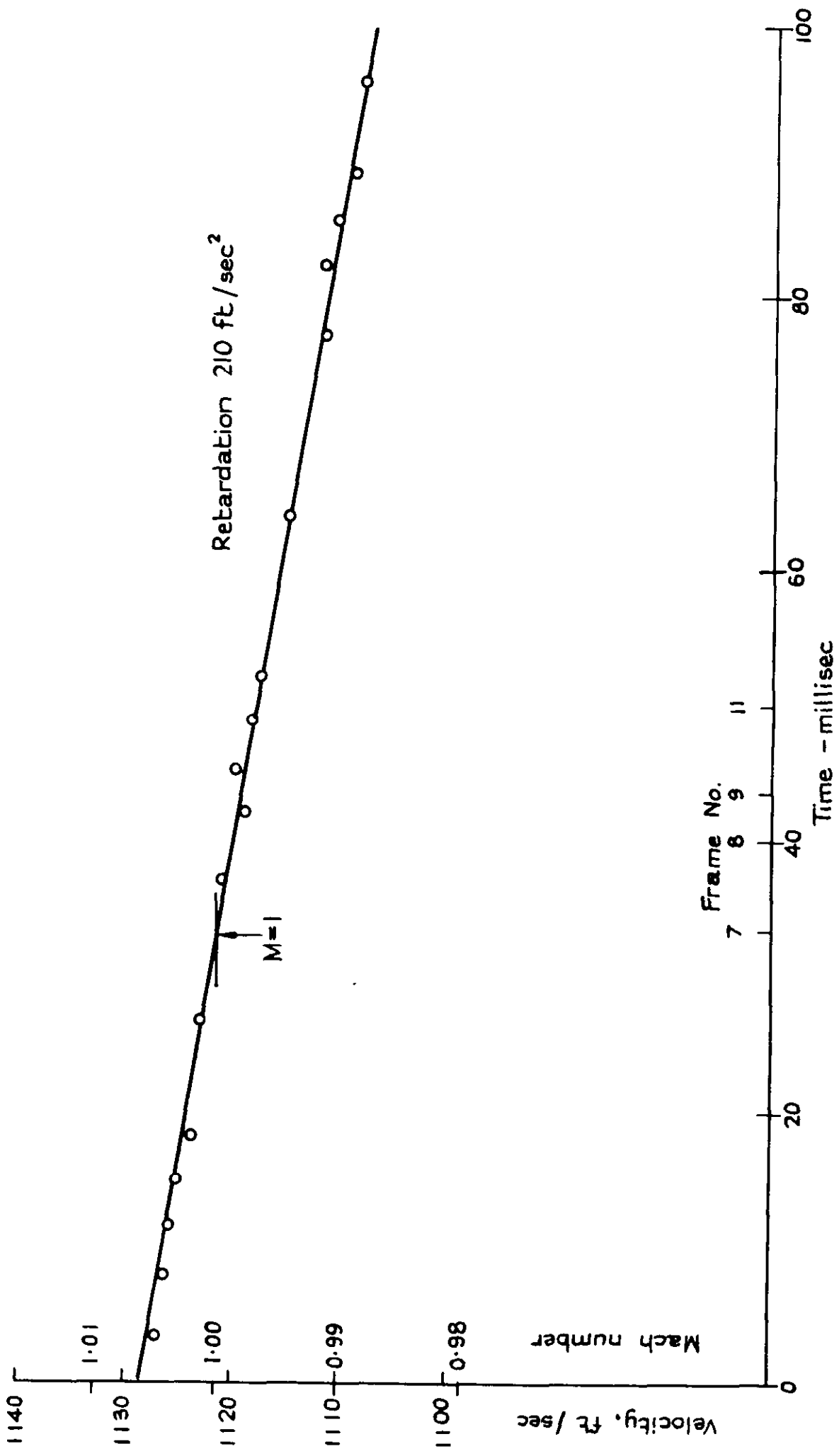
Fig. 28: Projectile N102, 3575 f.s., $M = 3.19$

Fig. 29.



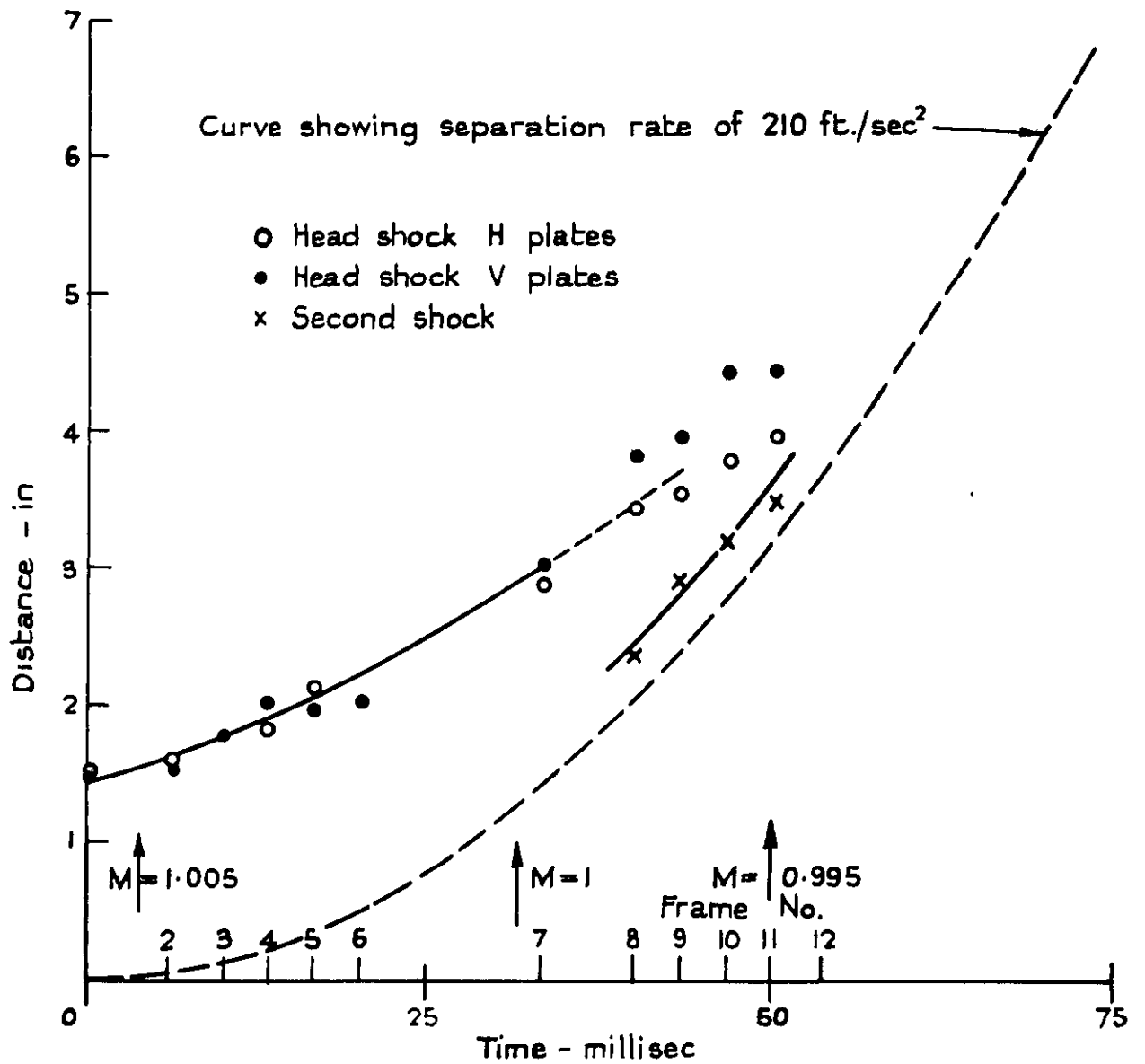
(a) Projectile F117

Fig. 30.

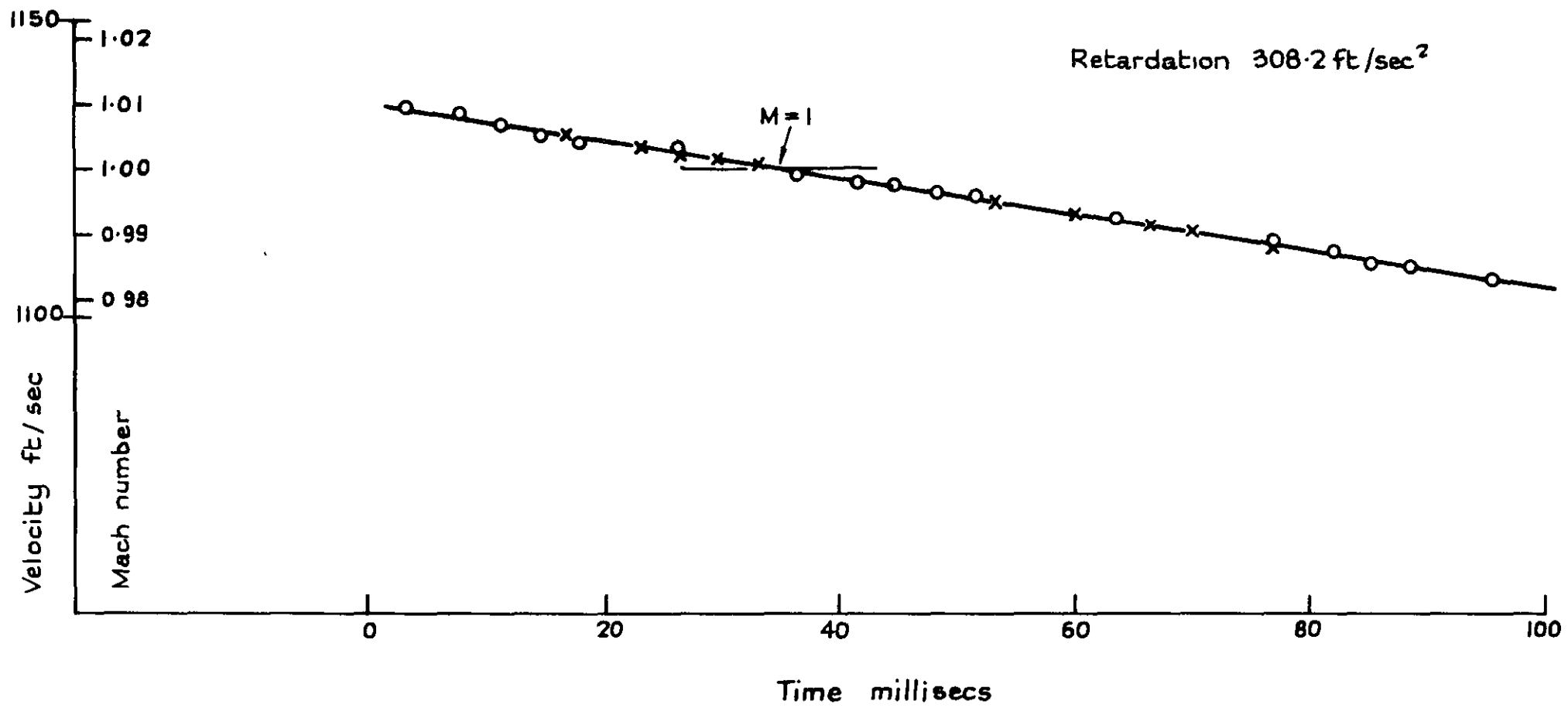


(b) Projectile F121

Fig. 31.



(c) F121 Distance of head shock from nose



Round No. F119

FIG. 32.

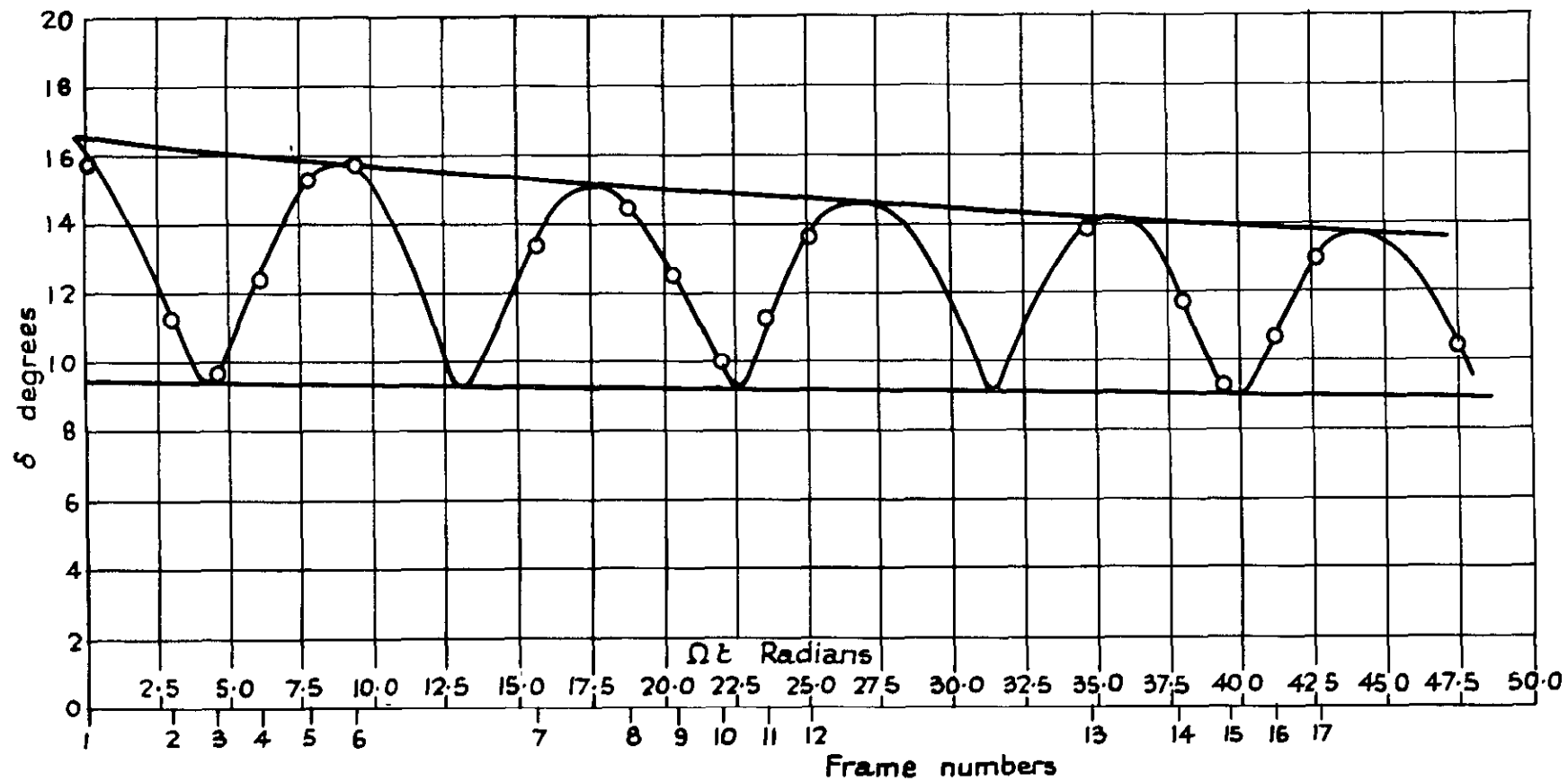
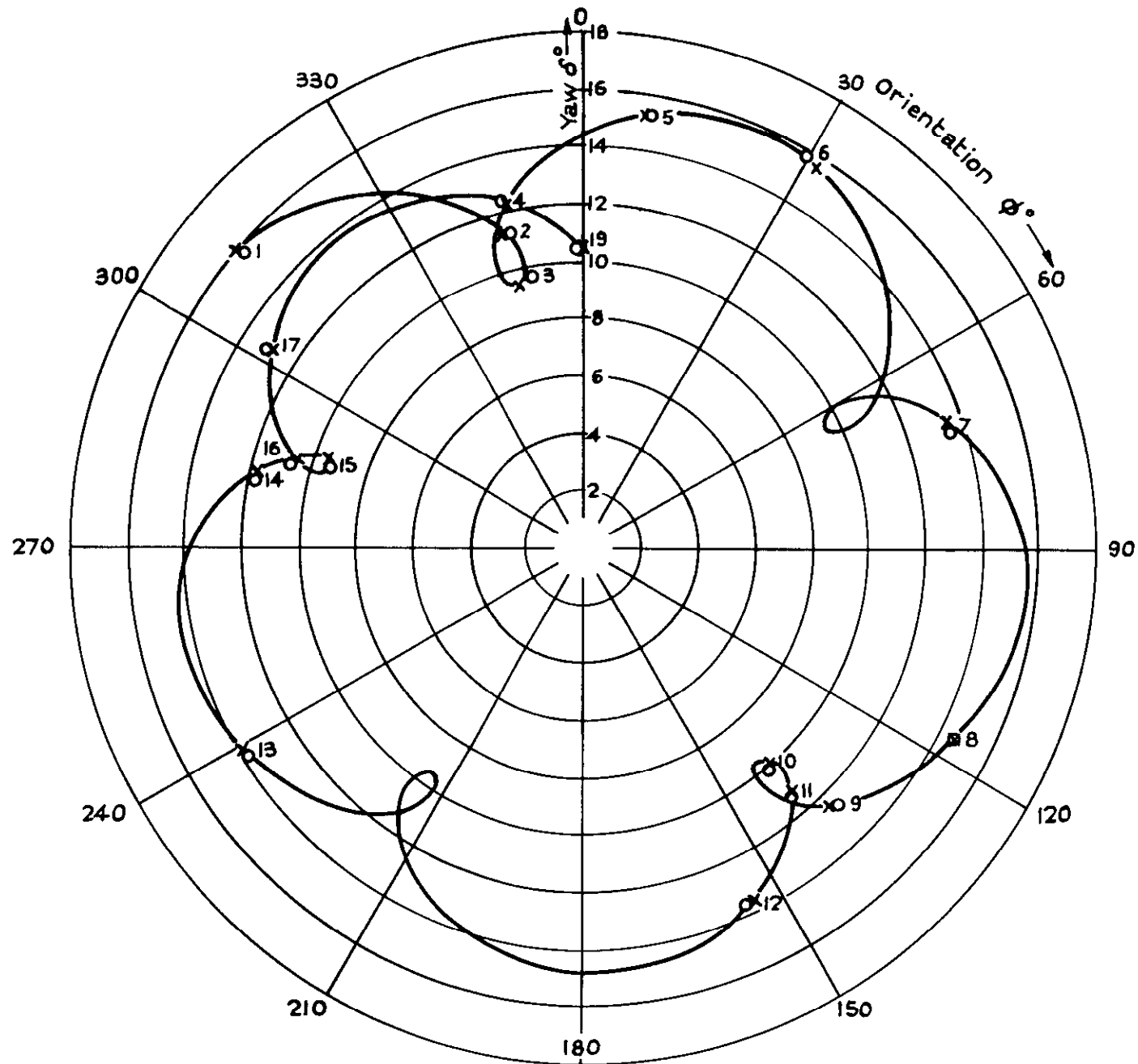


FIG. 33.

Round F119

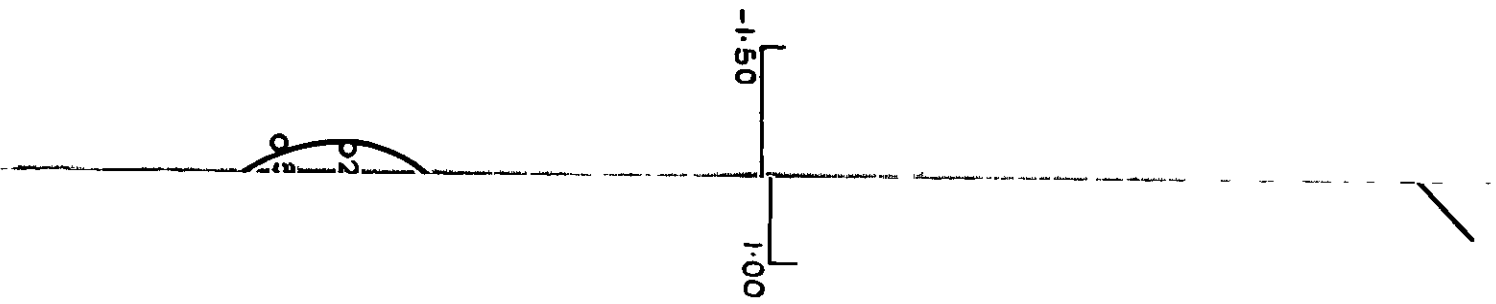


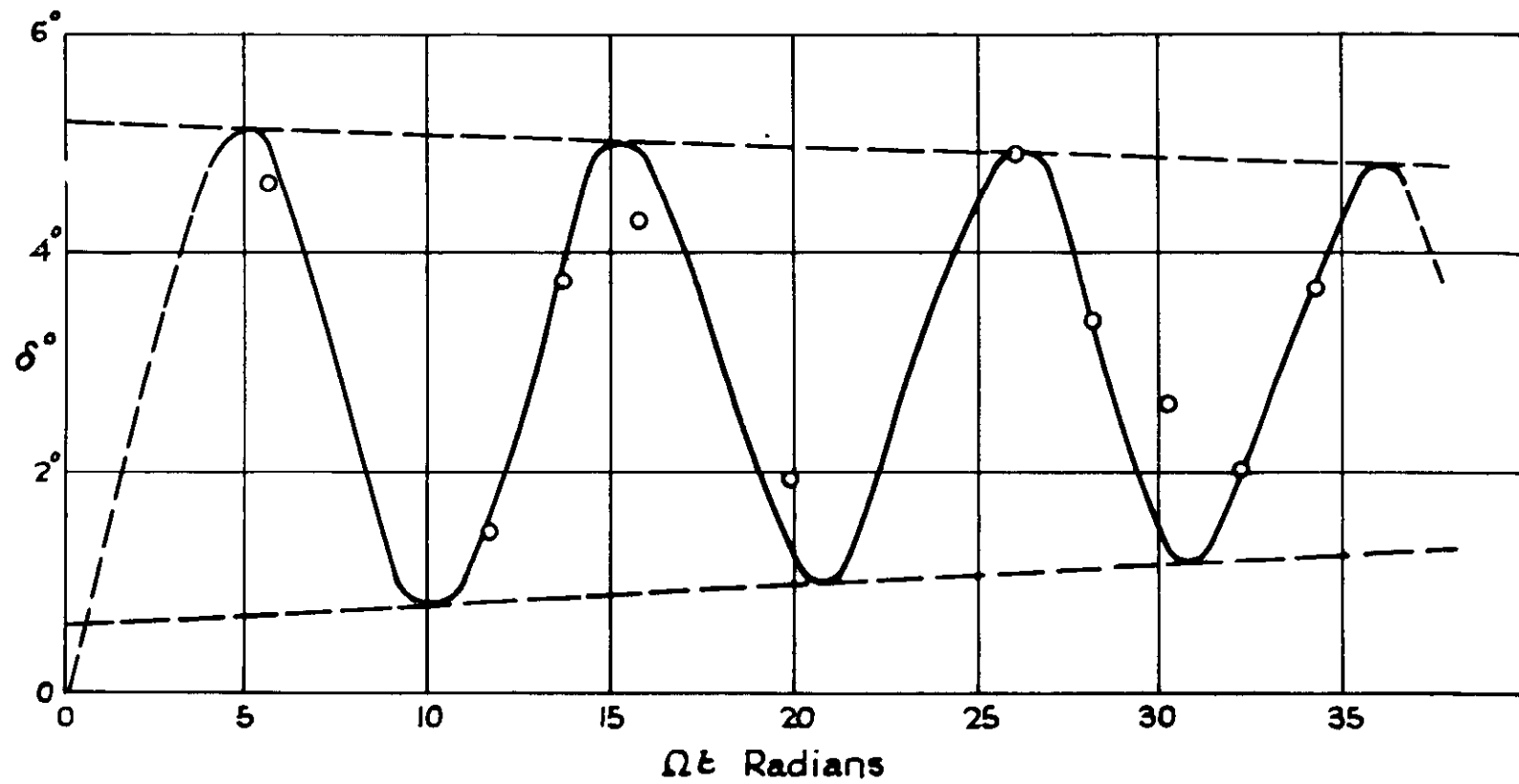
o Observed value
 x from analysis

FIG 34.

Round F119

Fig. 35.

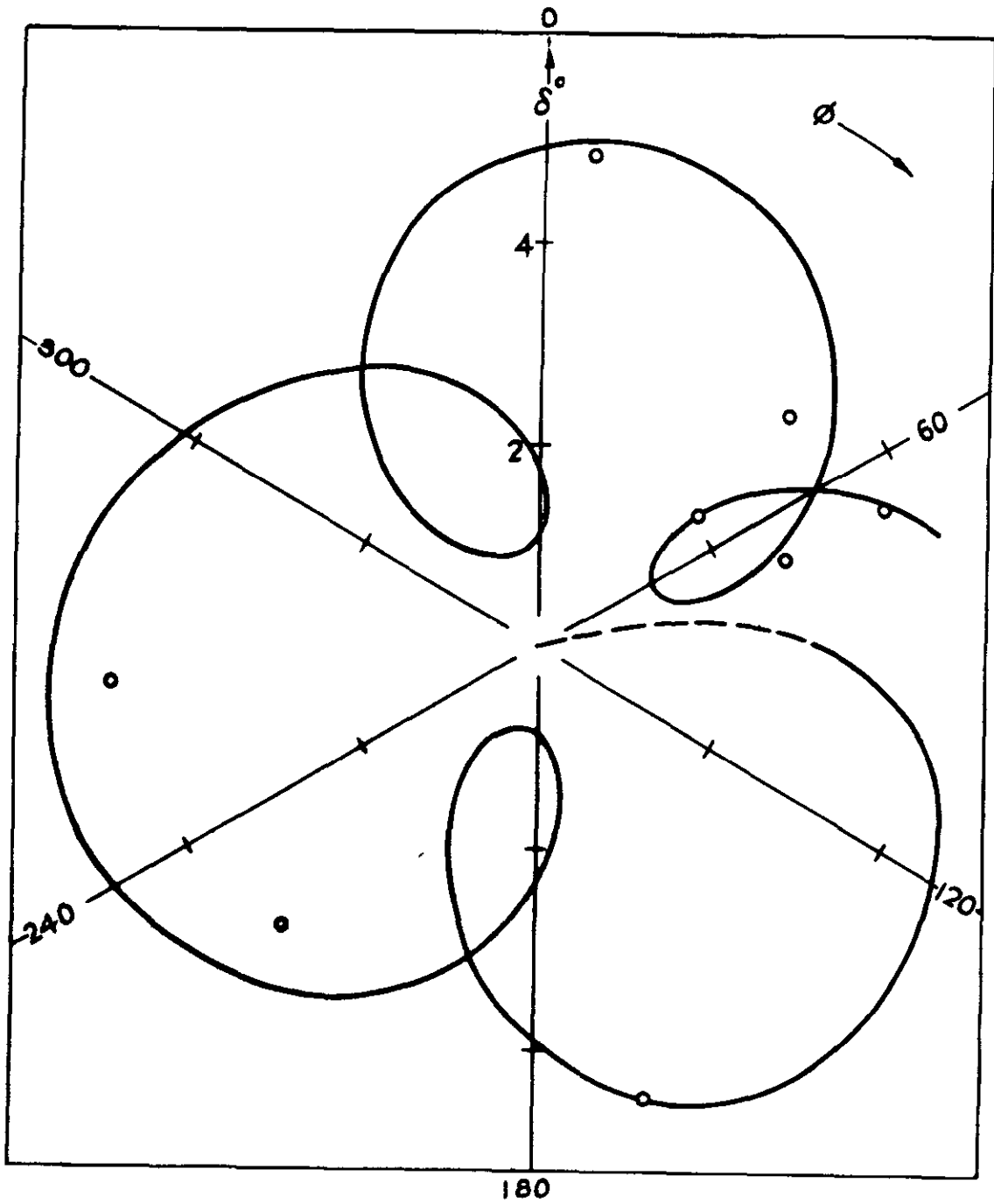




M.V. = 1,148 ft sec
 $\mathcal{M} = 1.01$

FIG. 36.

Fig. 37.



M.V. = 1,148 ft/sec
 $\mathcal{N} = 1.01$

FIGS 38 & 39.

FIG. 38.

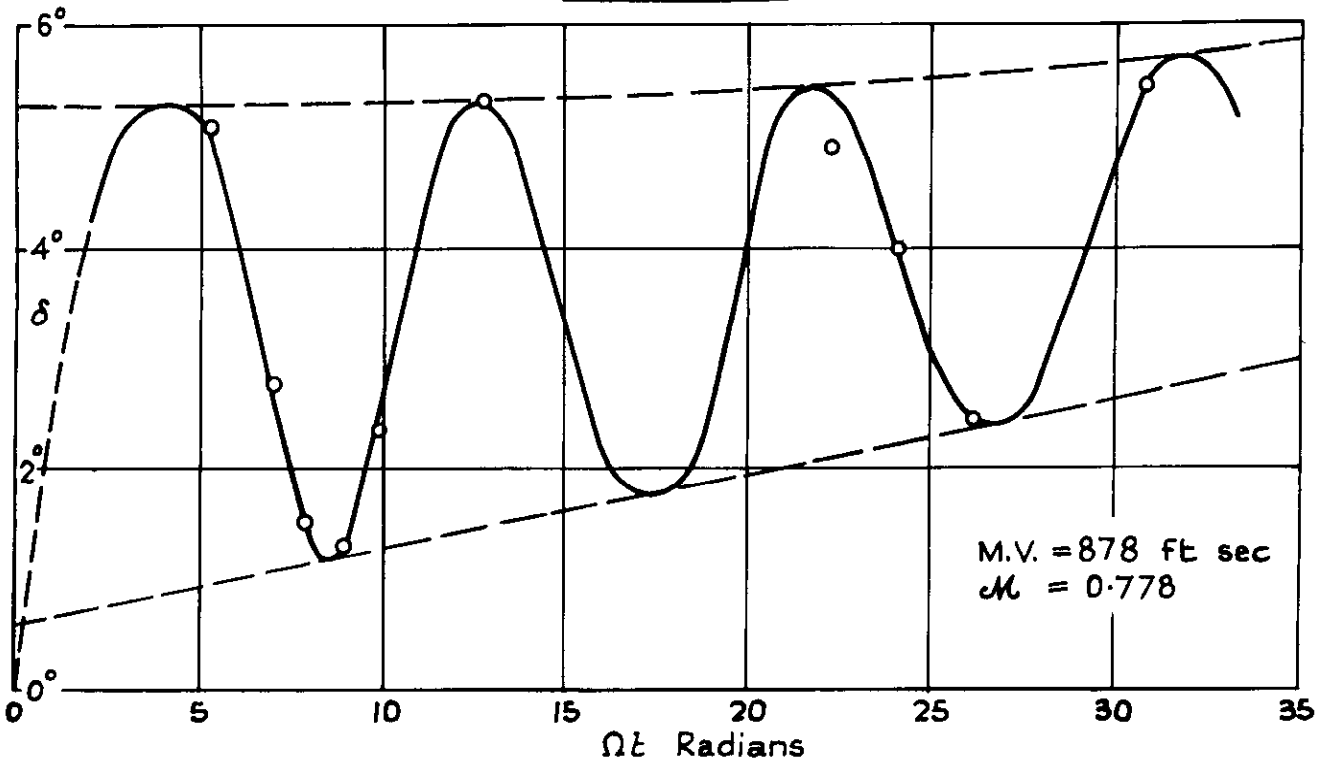
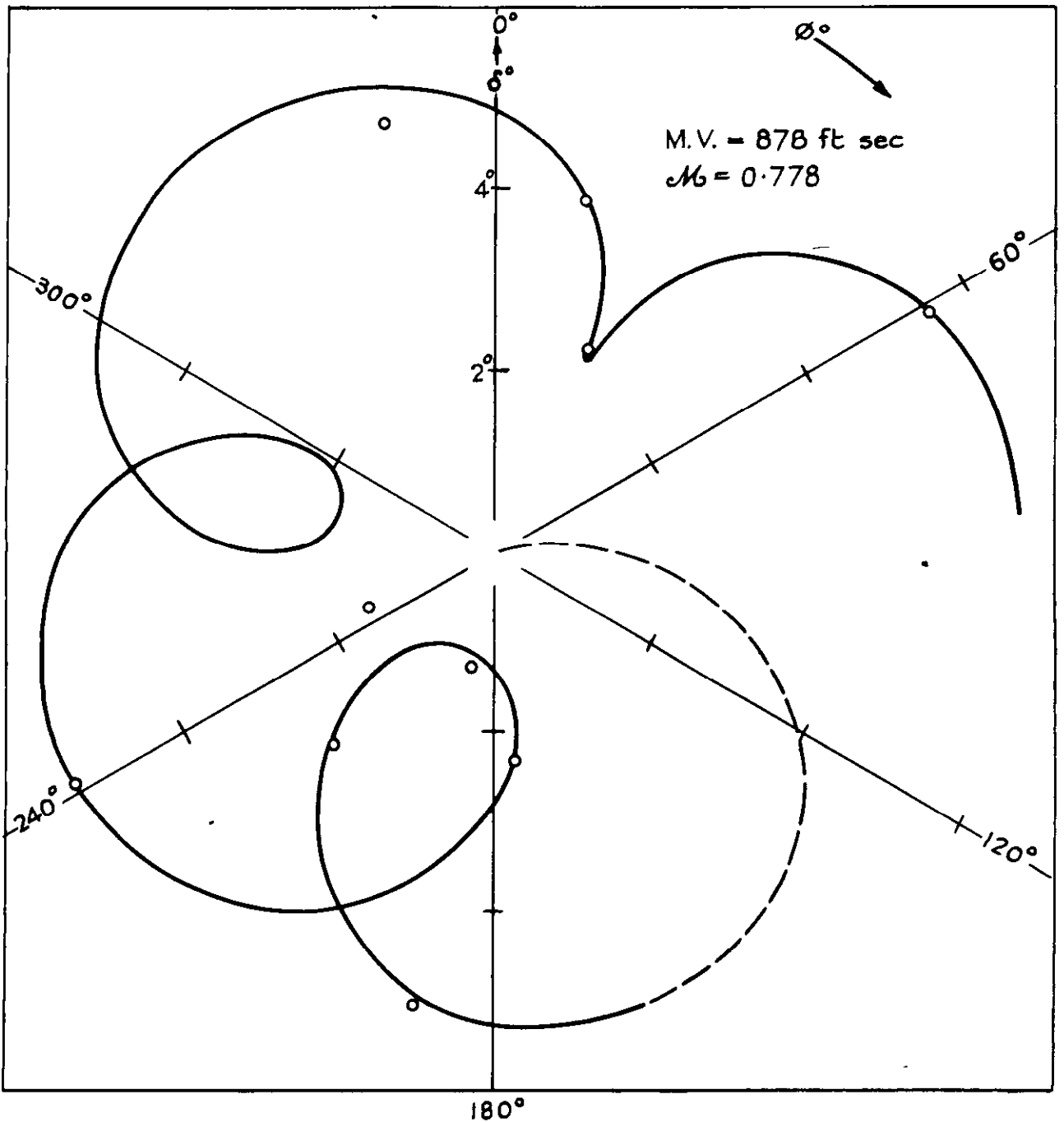


FIG. 39.



FIGS. 40 & 41

FIG. 40.

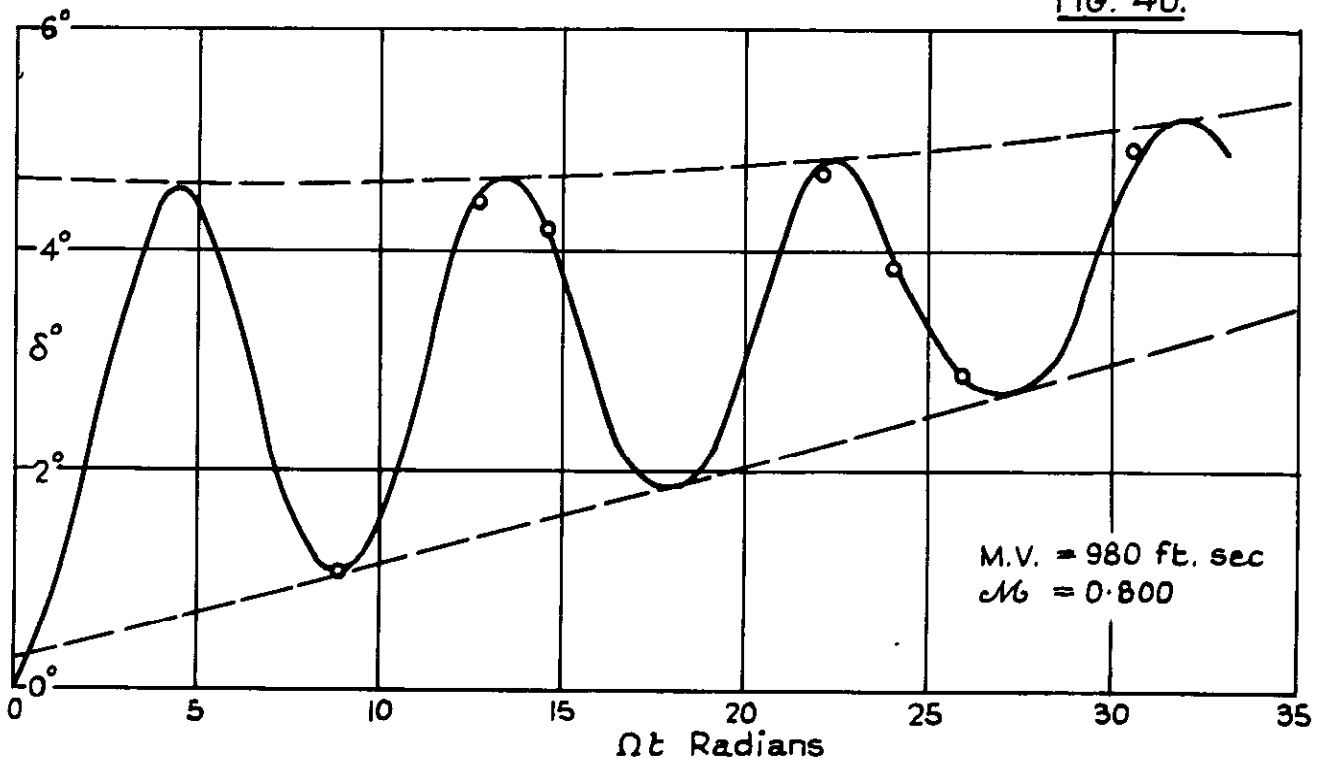


FIG. 41.

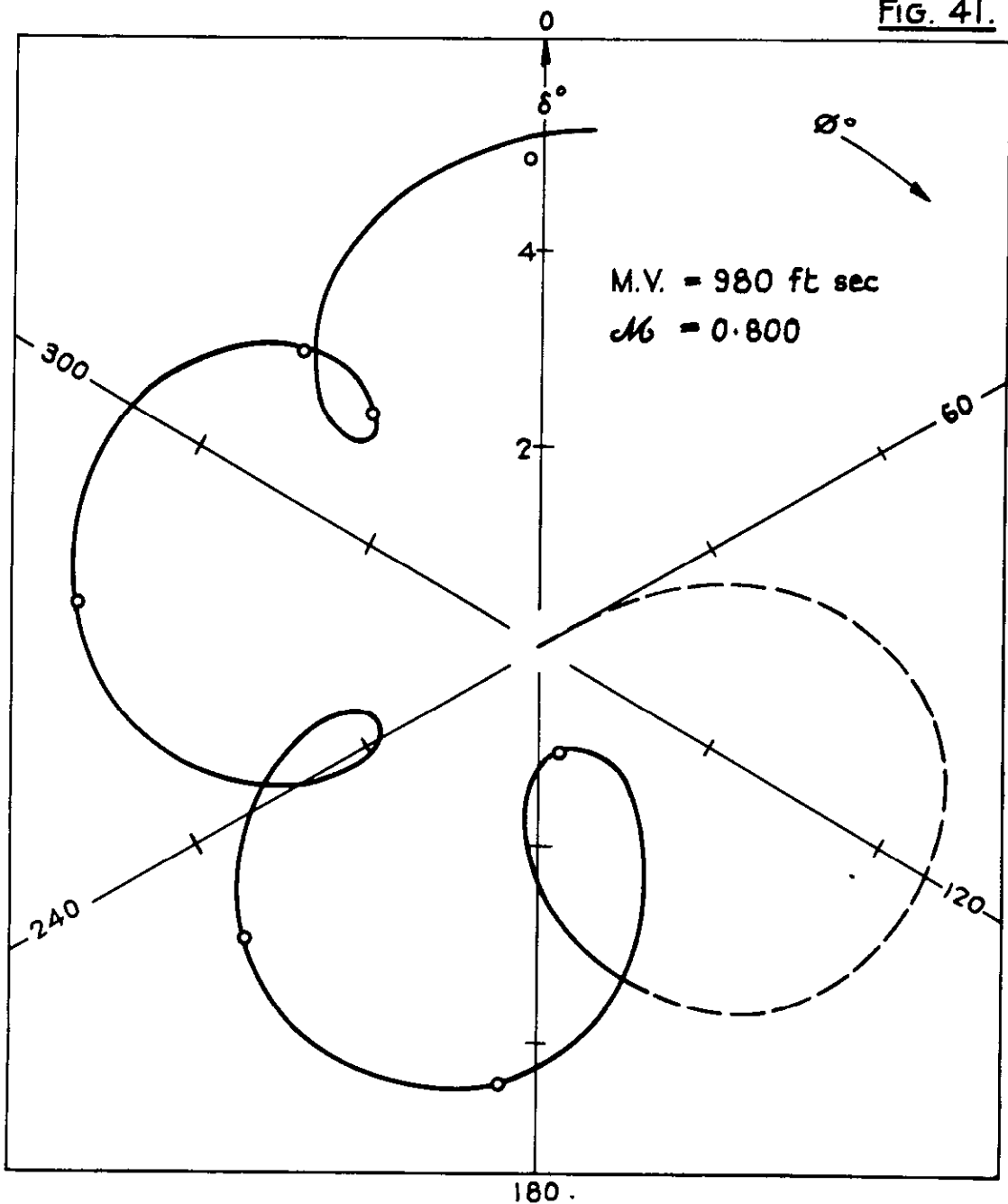


FIG. 42.

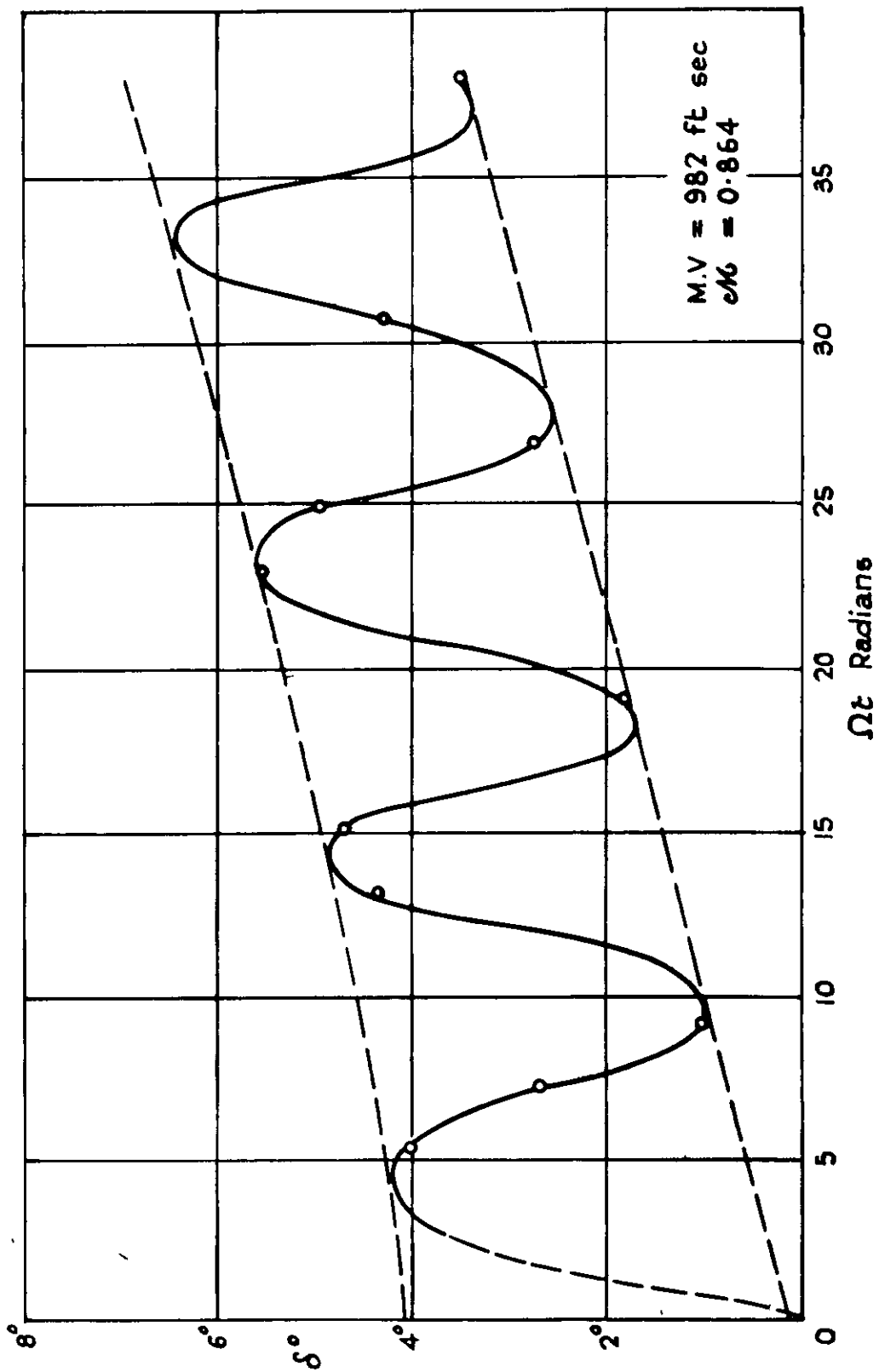
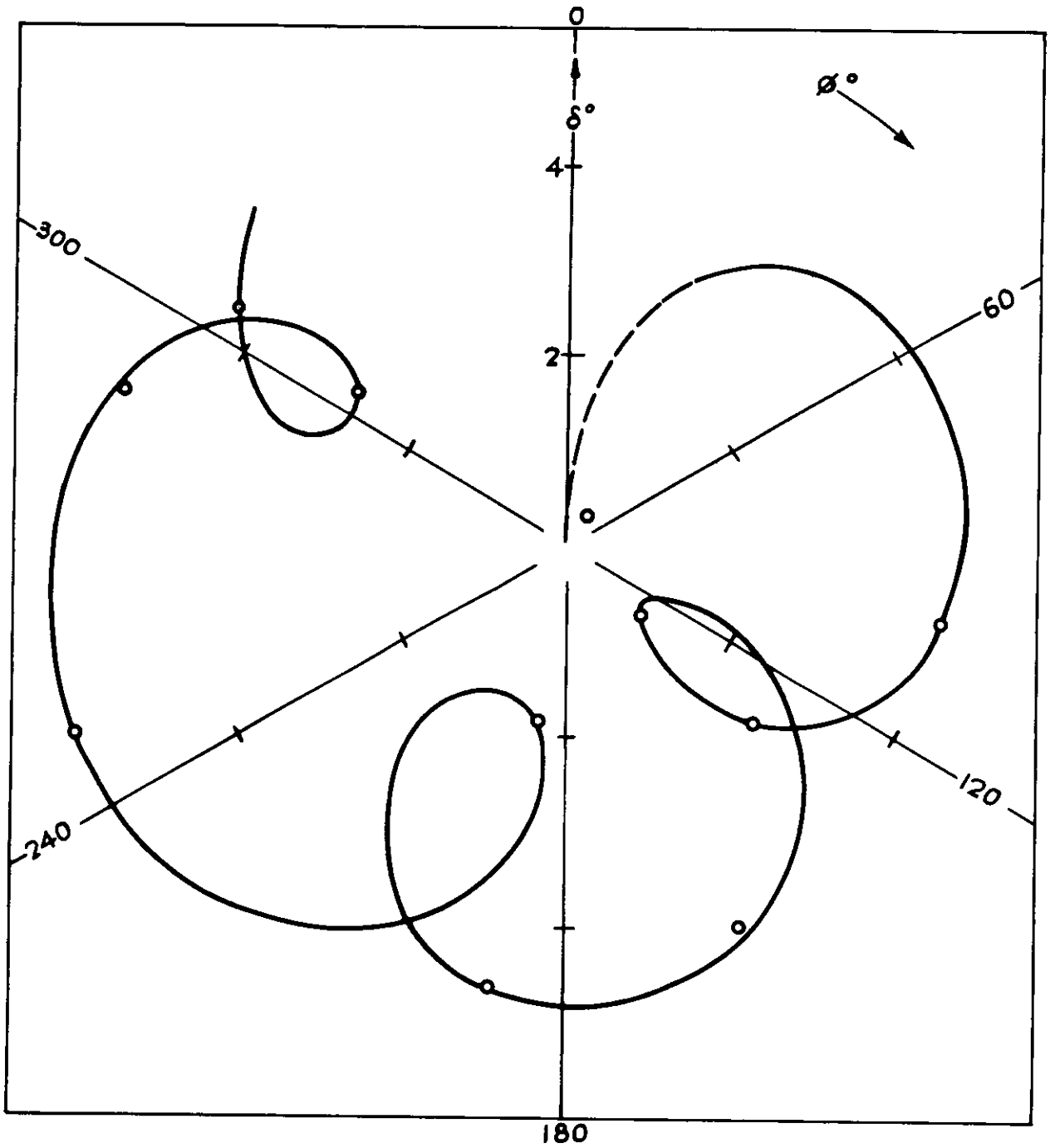


FIG. 43.

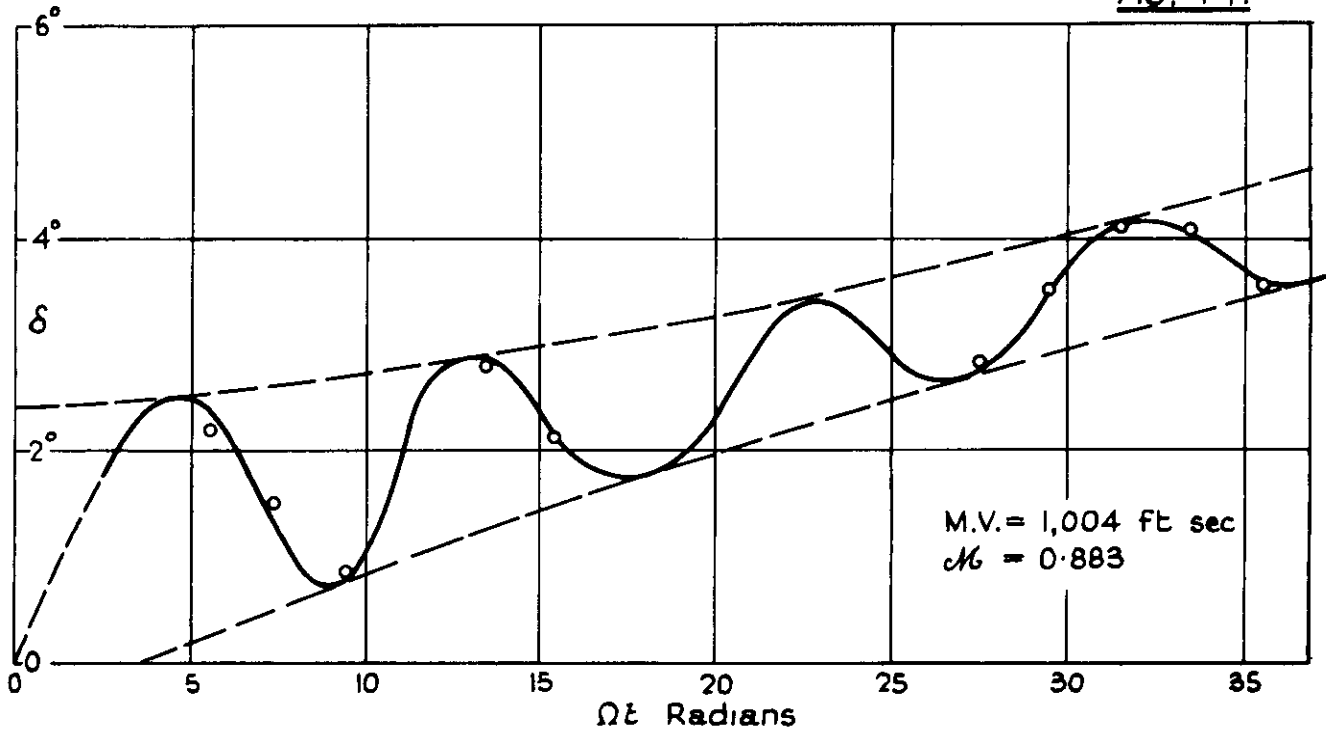
M.V. = 982 ft. sec.

$\mathcal{M} = 0.864$



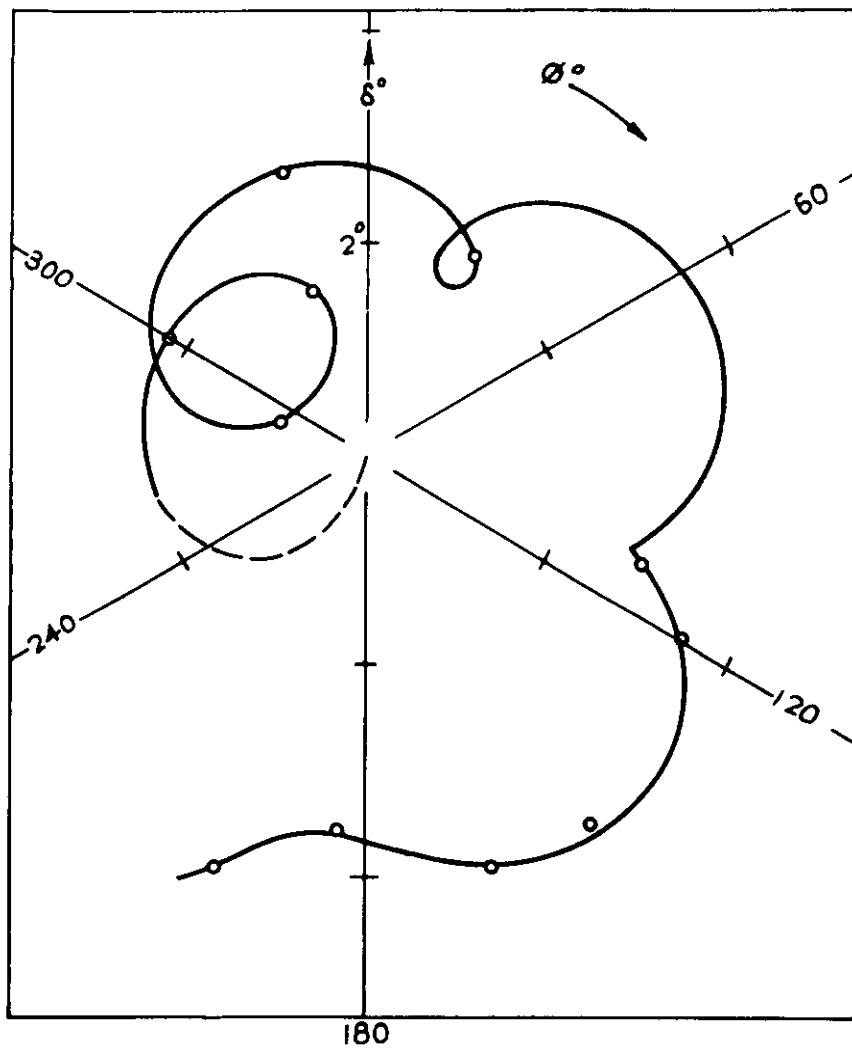
Figs 44 & 45.

FIG. 44.



M.V. = 1,004 ft sec
 $\mathcal{M} = 0.883$

FIG. 45.



CROWN COPYRIGHT RESERVED

PRINTED AND PUBLISHED BY HER MAJESTY'S STATIONERY OFFICE

To be purchased from

York House, Kingsway, LONDON, W C 2 423 Oxford Street, LONDON W 1

P O Box 569 LONDON, S E 1

13a Castle Street, EDINBURGH, 2 109 St Mary Street, CARDIFF

39 King Street MANCHESTER 2 Tower Lane, BRISTOL, 1

2 Edmund Street, BIRMINGHAM 3 80 Chichester Street, BELFAST

or from any Bookseller

1955

Price 5s 0d net

PRINTED IN GREAT BRITAIN